STRUCTURAL SYSTEMS

RESEARCH PROJECT

Report No.
SSRP–11/02

EVALUATION OF LONG-TERM PRESTRESS LOSSES IN POST-TENSIONED BOX-GIRDER BRIDGES

by

P. BENSON SHING

ALEXANDRA KOTTARI

Final Report Submitted to the California Department of Transportation under Contract No. 59A0420

March 2011

Department of Structural Engineering
University of California, San Diego
La Jolla, California 92093-0085

University of California, San Diego

Department of Structural Engineering

Structural Systems Research Project

Report No. SSRP–11/02

Evaluation of Long-Term Prestress Losses in Post-Tensioned Box-Girder Bridges

by

P. Benson Shing

Professor of Structural Engineering

Alexandra Kottari

Graduate Student Researcher

Final Report Submitted to the California Department of Transportation under Contract No. 59A0420

Department of Structural Engineering

University of California, San Diego

La Jolla, California 92093-0085

March 2011

Technical Report Documentation Page

1. Report No.	2. Government Accession No.	3. Recipient's Catalog No.
CA 11-0514		

4. Title and Subtitle	5. Report Date
Evaluation of Long-Term Prestress Losses in Post-Tensioned Box-Girder Bridges	March 2011
	6. Performing Organization Code
7. Author(s) P. Benson Shing and Alexandra Kottari	8. Performing Organization Report No. UCSD/SSRP-11/02
9. Performing Organization Name and Address Department of Structural Engineering School of Engineering University of California, San Diego La Jolla, California 92093-0085	10. Work Unit No. (TRAIS) 11. Contract or Grant No. 59A0420
12. Sponsoring Agency Name and Address California Department of Transportation Division of Engineering Services 1801 30th St., MS #9-2/5I Sacramento, California 95816	13. Type of Report and Period Covered Final Report 14. Sponsoring Agency Code

15. Supplementary Notes

Prepared in cooperation with the State of California Department of Transportation. This is the final report preceded by Report Nos. UCSD/SSRP-06/20 and UCSD/SSRP-06/21, which were all prepared for this project.

16. Abstract

Most of the recent highway bridges built in California have post-tensioned, cast-in-place, concrete box-girder superstructures rigidly connected to bridge columns. However, methods provided in the current (2007 and 2010) AASHTO LRFD Bridge Design Specifications for estimating long-term prestress losses are essentially based on research focused on pretensioned members and are not adequate for post-tensioned bridge girders. Long-term prestress losses in post-tensioned members are expected to be smaller than those in pretensioned members due to two main factors. One is the higher amount of mild reinforcement present in post-tensioned bridge girders, which provides a higher restraint to the creep and shrinkage of concrete, and the other is that post-tensioning could take place a long while after the girders have been cast and the concrete has reached a more mature age, which results in a lower creep. The main objectives of the study reported here were to assess the accuracy of the long-term prestress-loss estimation methods given in the current AASHTO LRFD Specifications for post-tensioned bridge girders, and to develop more suitable analysis methods for these members. One is a refined analysis method and the other is a simplified method also referred to as the approximate analysis method. Both methods have been validated and proven to be accurate using field data collected from two bridge structures that were monitored for prestress losses over a period of more than four years. Furthermore, formulas recommended in the AASHTO 2004 and 2007 Specifications for calculating the creep and shrinkage of concrete have been evaluated with the material data obtained from concrete cylinders cast with the same batches of concrete used for the monitored bridge girders, and have been used for the loss calculations. It has been found that the formulas in AASHTO 2004 provide a much better correlation with the creep and shrinkage data obtained from the concrete cylinders than AASHTO 2007. In general, the AASHTO 2007 formulas significantly under-estimate the creep and shrinkage of the concrete cylinders, and, thereby, result in calculated long-term losses that are much lower than the measured values. Hence, the creep and shrinkage formulas provided in AASHTO 2004 are recommended for the prestress-loss calculations using the proposed refined analysis method. Finally, suggestions are provided for possible implementation of the proposed analysis methods in the AASHTO LRFD Specifications for calculating long-term prestress losses in post-tensioned bridge girders. Both methods are expressed in forms that can be readily implemented in the AASHTO LRFD Specifications.

17. Key Words	18. Distribution Statement
Box girders, Bridges, Cast-in-place, Concrete, Creep, Post-tensioned, Prestress, Prestress losses, Relaxation, Shrinkage, Steel tendons	No restrictions. This document is available to the public through the National Technical Information Service, Springfield, Virginia 22161.

19. Security Classification (of this report)	20. Security Classification (of this page)	21. No. of Pages	22. Price
Unclassified	Unclassified	74	

Form DOT F 1700.7 (8-72) Reproduction of completed page authorized

DISCLAIMER

This document is disseminated in the interest of information exchange. The contents of this report reflect the views of the authors who are responsible for the facts and accuracy of the data presented herein. The contents do not necessarily reflect the official views or policies of the State of California or the Federal Highway Administration. This publication does not constitute a standard, specification or regulation. This report does not constitute an endorsement by the California Department of Transportation of any product described herein.

For individuals with sensory disabilities, this document is available in Braille, large print, audiocassette, or compact disk. To obtain a copy of this document in one of these alternate formats, please contact: the Division of Research and Innovation, MS-83, California Department of Transportation, P.O. Box 942873, Sacramento, CA 94273-0001.

ACKNOWLEDGMENTS

This study was supported by the California Department of Transportation (Caltrans) and was the last phase of a project aimed at developing improved analytical methods to estimate long-term prestress losses in post-tensioned bridge girders. Professor Vistasp Karbhari at the University of Alabama, Huntsville (formerly at the University of California, San Diego) was the original principal investigator of this project. The authors would like to thank him and his previous graduate student researcher, Dr. Seung Dae Kim, for their crucial contributions to this project and for providing the long-term prestress loss data collected from two bridge structures to validate the analytical models presented in this report. The authors would also like to thank the technical staff of the Powell Structural Engineering Laboratories at the University of California, San Diego for their efforts in instrumenting the two monitored bridge structures and collecting the field data. Finally, the authors are most grateful to Charles Sikorsky, Susan Hida, Marc Friedheim, and Traci Menard of Caltrans for their input and continuous support throughout this project.

ABSTRACT

Most of the recent highway bridges built in California have post-tensioned, cast-in-place, concrete box-girder superstructures rigidly connected to bridge columns. However, recommendations in the current AASHTO LRFD Bridge Design Specifications (2007 and 2010) for calculating long-term prestress losses are essentially developed for pretensioned members and are not adequate for post-tensioned bridge girders. Long-term prestress losses in post-tensioned members are expected to be smaller than those in pretensioned members due to two main factors. One is the higher amount of mild reinforcement present in post-tensioned bridge girders, which provides a higher restraint to the creep and shrinkage of concrete, and the other is that post-tensioning could take place a long while after the girders have been cast and the concrete has reached a more mature age, which results in a lower creep. While the latter factor is accounted for in the refined analysis method of the current AASHTO Specifications, neither is considered in AASHTO's approximate analysis method. Furthermore, the formulas for estimating the creep and shrinkage of concrete in the 2007 and 2010 Specifications have been changed from those in the 2004 Specifications. These new formulas have been essentially calibrated with high-strength concrete, which is nowadays widely used for pretensioned bridge girders but not for post-tensioned bridge girders. The main objectives of the study reported here were to assess the accuracy of the long-term prestress-loss estimation methods given in the current AASHTO LRFD Specifications for post-tensioned bridge girders, and to develop more suitable analysis methods for these members.

As a result of this study, two analysis methods are proposed here for post-tensioned bridge girders. One is a refined analysis method and the other is a simplified method also referred to as the approximate method. Both methods have been validated and proven to be accurate using field data collected from two bridge structures that were monitored for long-term prestress losses over a period of more than four years.

Furthermore, formulas recommended in the AASHTO 2004 and 2007 Specifications for estimating the creep and shrinkage of concrete have been evaluated with the material data obtained from concrete cylinders cast with the monitored bridge girders, and have been used to calculate long-term prestress losses in these bridge structures. It has been found that the formulas in AASHTO 2004 provide a much better correlation with the creep and shrinkage data obtained from the concrete cylinders than those in AASHTO 2007. The AASHTO 2007 formulas

significantly under-estimate the creep and shrinkage of the concrete cylinders, and lead to much lower calculated long-term losses as compared to the actual losses measured from the bridges and those calculated with the AASHTO 2004 creep and shrinkage formulas.

Finally, suggestions are provided for possible implementation of the proposed analysis methods in the AASHTO LRFD Specifications for estimating long-term prestress losses in post-tensioned bridge girders. Both methods are formulated in forms similar to those adopted in the current AASHTO LRFD Specifications for pretensioned girders.

TABLE OF CONTENTS

1 Introduction

Most of the recent highway bridges built in California have post-tensioned, cast-in-place, concrete box-girder superstructures rigidly connected to bridge columns. Prestressed concrete members experience prestress losses over time due to the creep and shrinkage of concrete and the stress relaxation in the prestressing steel. To have durable and economical bridge structures with good serviceability, an accurate estimation of the long-term losses is important in the design process. However, recommendations in the current AASHTO LRFD Bridge Design Specifications (2007 and 2010) for calculating long-term prestress losses are essentially developed for pretensioned girders and are not adequate for post-tensioned bridge girders. In addition to a lump-sum method, the current AASHTO LRFD Specifications provide two analysis methods for calculating long-term losses in pretensioned bridge girders. One is a refined method and the other is a simplified method, which is referred to as the approximate method in the specifications. While the refined method is also permitted for post-tensioned members, both methods are based on research data derived from pretensioned bridge girders (Tadros et al. 2003). Long-term prestress losses in post-tensioned members are expected to be smaller than those in pretensioned members due to two main factors. One is the higher amount of mild reinforcement present in post-tensioned bridge girders, which provides a higher restraint to the creep and shrinkage of concrete, and the other is that post-tensioning could take place a long while after the girders have been cast and the concrete has reached a more mature age, which results in a lower creep. While the latter factor is accounted for in the refined analysis method of the current AASHTO Specifications, neither is considered in AASHTO's approximate analysis method. Furthermore, the formulas for estimating the creep and shrinkage of concrete in the 2007 and 2010 Specifications have been changed from those in the 2004 Specifications. These new formulas have been essentially calibrated with high-strength concrete, which is nowadays widely used for pretensioned bridge girders but not for post-tensioned bridge girders.

Youakim and Karbhari (2006) have proposed a refined analysis method for calculating long-term prestress losses in post-tensioned members with the consideration of the influence of the mild reinforcement. To validate the method, long-term prestress losses in two bridge structures were monitored (Lewis and Karbhari 2006; Kim 2009). One bridge is located in a coastal area in San Diego, California, and the other is in an inland location in Riverside, California.

The main objectives of the study reported here were to assess the accuracy of the long-term prestress-loss estimation methods given in the current AASHTO LRFD Specifications for post-tensioned bridge girders, to evaluate the refined analysis method proposed by Youakim and Karbhari using field data collected from the two aforementioned bridges, and to develop a refined analysis method and an approximate analysis method that can be readily implemented in the AASHTO LRFD Specifications for post-tensioned members. To this end, the monitored bridge structures are briefly described (Chapter 2) in this report; formulas recommended in the AASHTO 2004 and 2007 LRFD Specifications for calculating the creep and shrinkage of concrete are evaluated with the material test data collected from concrete cylinders cast with the monitored bridge structures (Chapter 3); the method proposed by Youakim and Karbhari is evaluated with the field data, and a new refined analysis method, which has a form similar to that of the refined method in the current AASHTO LRFD Specifications, has been developed and validated (Chapter 4); an approximate analysis method that considers the presence of mild reinforcement and the age of concrete at prestressing has been developed and validated (Chapter 5); and finally, suggestions for possible implementation of the proposed analysis methods in the AASHTO LRFD Specifications are provided (Chapter 6).

2 Monitored Bridges

In this chapter, the two bridge structures, namely, the I5-I805 connector in San Diego and the I215-CA91 connectors in Riverside, California, monitored by Lewis and Karbhari (2006) and Kim (2009) for long-term prestress losses are described. The prestress-loss and material data collected from these bridges will be used to evaluate the long-term loss calculation methods presented in Chapters 4 and 5 of this report. In this chapter, the main features of the bridge structures, the essential design details, and the local climate conditions are presented; the timeline of the construction process is summarized; and the material tests, including the creep and shrinkage measurements, conducted on concrete cylinders cast together with the monitored bridge girders, are described. More detailed information on the bridge construction, instrumentation of the monitored bridge spans, measuring procedures, and material testing can be found in Lewis and Karbhari (2006) and Kim (2009).

2.1 I5-I805 Truck Connector Frames 4 and 5

The I5-I805 truck connector is a continuous bridge with six frames, which is located in a coastal area in San Diego, California. The location is close to the UC-San Diego campus and has a mild climate and a year-round average relative humidity of 64-67%. The connector has a post-tensioned, cast-in-place, continuous box girder consisting of three cells, with a typical cross section depicted in Fig. 2.1. The monitored bridge segments are in Frames 4 and 5 of the connector. Frame 4 comprises Spans 12, 13 and 14, and Frame 5 has Spans 15, 16, and 17 according to the design drawings. Each of Spans 13 and 16 has two sections instrumented to monitor prestress losses, with one at midspan and the other next to a bent. Span 13 has a length of 80.62 m and Span 16 is 52.82 m long as shown in Fig. 2.2.

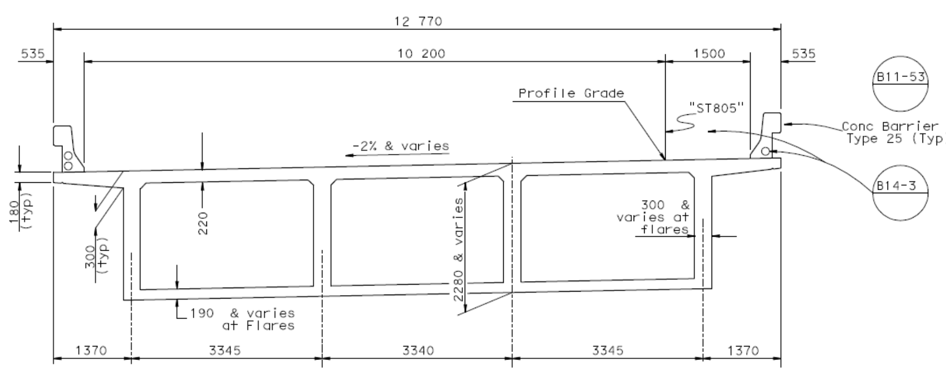

Fig. 2.1 –Typical box-girder cross section in I5-I805 (Caltrans Design Drawings)

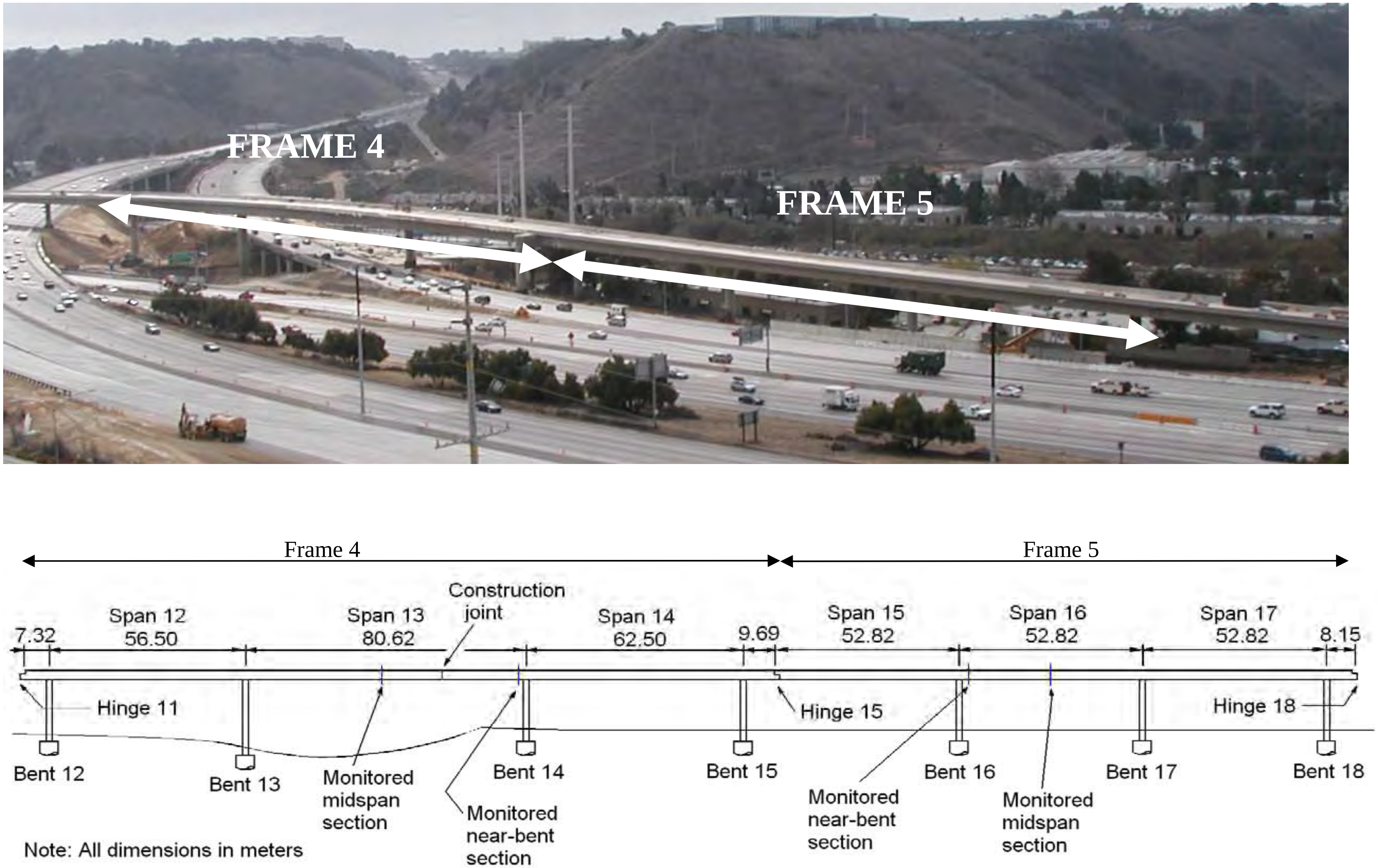

Fig. 2.2 – I5-I805 bridge elevation view and monitored sections (Kim 2009)

The girder in Frame 4 was constructed in three stages. The soffit and webs were cast on October 5 and November 2, 2004, respectively, while the deck was poured on March 3, 2005. Prestressing took place on March 29, 2005, and the falsework was removed on July 22, 2005. The girder in Frame 5 was cast in two stages. The soffit and webs were cast on April 5, 2005, and the deck on May 3, 2005. Prestressing occurred on May 20, 2005, and the falsework was removed on July 29 of the same year. These dates are summarized in Tables 2.1 and 2.2.

Table 2.1 - Construction time log and age of concrete at loading event for Frame 4

Loading event (Date)	Casting dates and concrete age (in days) at loading		
	Soffit (10/5/04)	Web (11/2/04)	Deck (3/3/05)
Prestressing (3/29/05)	175	147	26
Removal of falsework (7/22/05)	290	262	141

Table 2.2 - Construction time log and age of concrete at loading event for Frame 5

Loading event (Date)	Casting dates and concrete age (in days) at loading	
	Soffit and Web (4/5/05)	Deck (5/3/05)
Prestressing (5/20/05)	45	17
Removal of falsework (7/29/05)	115	87

The prestressing strand used in I5-I805 is Grade 270 (1,860 MPa tensile strength) with a nominal yield strength of 230 ksi (1586 MPa). The modulus of elasticity of the prestressing steel is assumed to be 28,000 ksi (193 GPa) in this study. The prestressing forces in Span 13 (Frame 4), after immediate losses, are 11,648 kips (51,835 kN) at midspan and 11,715 kips (52,131 kN) near the bent. The prestressing forces in Span 16 (Frame 5) are 7,560 kips (33,641 kN) and 7,874 kips (35,040 kN) at midspan and near the bent, respectively.

The mild reinforcement used in the bridge is Grade 60. At each section of the two monitored spans, the total cross-sectional area of the mild reinforcement is 56.42 in.^{2} (364 cm^2) in the top flange and 48.21 in.^{2} (311 cm^2) in the bottom flange. Small quantities of mild reinforcement are also present in the webs. The elevation and cross-sectional view of the girders monitored for prestress losses in the I5-I805 connector are shown in Figs. 2.3 and 2.4. This information was obtained by Kim (2009) based on the bridge plans provided by Caltrans.

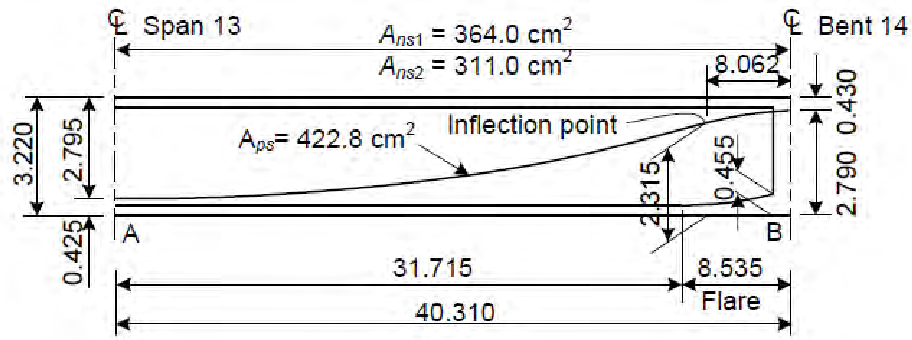

(a) Half elevation view

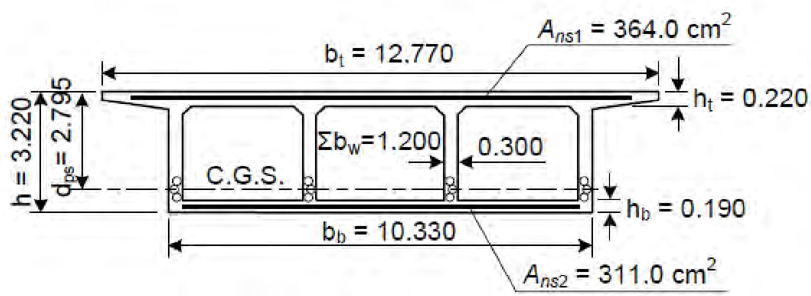

(b) Cross section at midspan

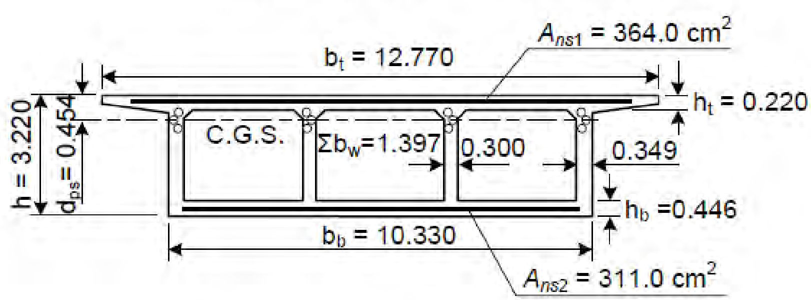

(c) Cross section near bent

Fig. 2.3 – Half elevation and cross-sectional views of girder in Frame 4 on I5-I805 (Kim 2009)

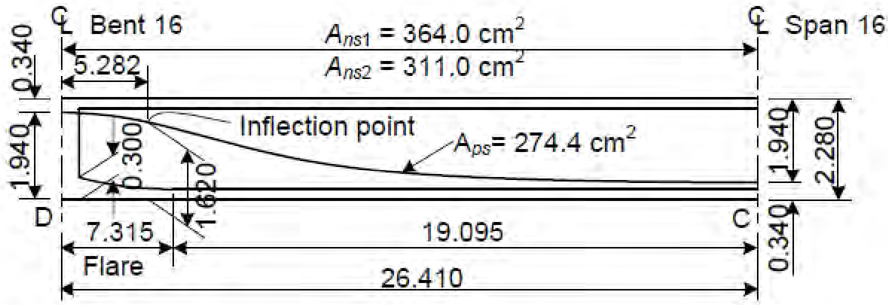

(a) Half elevation view

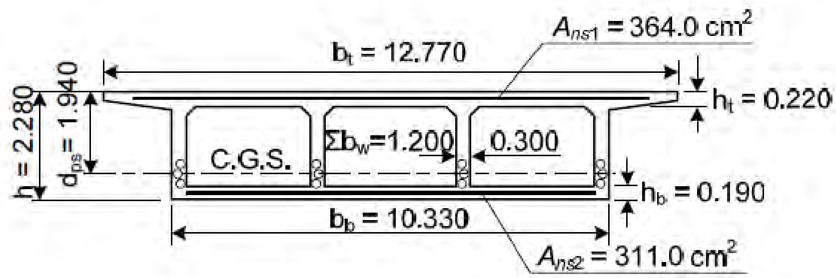

(b) Cross section at midspan

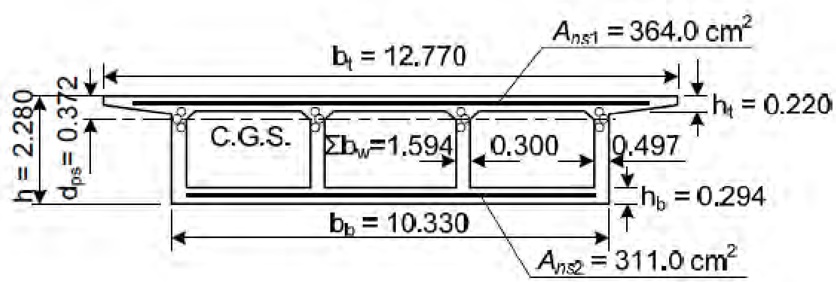

(c) Cross section near bent

Fig. 2.4 – Half elevation and cross-sectional views of girder in Frame 5 on I5-I805 (Kim 2009)

The cross-sectional areas of the girder in Frame 4 are 12,617 in.^{2} (8.14 m^2) at midspan and 16,926 in.^{2} (10.92 m^2) near the bent. For the girder in Frame 5, the respective areas are 10,881 in.^{2} (7.02 m^2) and 13,423 in.^{2} (8.66 m^2).

Material tests were conducted on concrete cylinders cast with the bridge girders to obtain the creep coefficients and shrinkage strains as a function of time. To this end, on each of the concrete pour days, as presented in Tables 2.1 and 2.2, concrete cylinders were cast using the same batch of concrete used for the girder. The specimens were then transferred to the UC-San

Diego campus, which is close to the bridge site, so that the specimens were kept under similar environmental conditions as the bridge. The cylinders were 12 x 6 in. (300 x 150 mm). To simulate the actual curing conditions of the bridge, the specimens were moist cured at an ambient temperature of around 59°F (15 °C) for a period of seven days after casting.

For each batch of concrete, the specimens were divided into three sets. One set was not loaded and was used for measuring shrinkage. To measure the shrinkage strain, mechanical (DEMEC) gage points were attached to the concrete cylinders. The shrinkage of the cylinders was determined from the measured free shrinkage by removing the temperature effect using the measured temperature.

The second set was subjected to a constant stress of 30% of the expected 28-day concrete compressive strength, and it was used for the determination of the creep property. The load was applied on the same day on which the girder was prestressed. The specimens were loaded to the desired stress level with the use of a hydraulic jack and the load was maintained in a load frame by an elastic spring. DEMEC points were used for the strain measurement. The strain readings were influenced by creep, shrinkage, and temperature effects. Thus, the actual creep strain was calculated by removing the shrinkage strain, elastic strain, and temperature effects from the measured strains. The creep coefficient was calculated as the ratio of the creep strain to the initial elastic strain.

Creep and shrinkage data were collected at regular time intervals, starting from the day of prestressing. Some shrinkage data were also collected before prestressing. The shrinkage strains and creep coefficients obtained from the specimens are presented in Section 3.3 of this report.

The third set of specimens was used for obtaining the compressive strengths and the modulus of elasticity. For Frame 4, these tests took place on April 8, 2005, and July 25, 2005, shortly after the prestressing of the tendons and the removal of falsework, respectively. For Frame 5, the specimens were tested on May 20, 2005, and July 25, 2005. The average concrete strengths obtained are summarized in Tables 2.3 and 2.4. Furthermore, a weighted-average concrete strength was calculated for each batch based on the respective cross-sectional areas of the deck and soffit of the bridge sections. The weighed-average concrete strengths obtained for the girder sections are presented in Table 2.5. Concrete strengths at 28 days are not available from the data base. However, they could be slightly lower if not close to the strengths obtained on the aforementioned days. The AASHTO 2004 formula for the calculation of creep coefficients has a factor considering the 28-day strength of concrete. Using the compressive strength of concrete at the time of prestressing, which was longer than 28 days, in the calculation could result in a slightly lower creep and prestress loss.

Table 2.3 - Test dates and concrete compressive strengths in ksi (MPa) for Frame 4

Test Date	Loading event (Date)	Soffit cast on 10/05/04	Web cast on 11/2/04	Deck cast on 3/3/05
4/8/2005	Prestressing (03/29/05)	5.94 (40.93)	6.23 (42.96)	4.55 (31.38)
7/25/2005	Removal of falsework (7/22/05)	5.86 (40.37)	6.13 (42.24)	5.39 (37.15)

Table 2.4 - Test dates and concrete compressive strengths in ksi (MPa) for Frame 5

Test Date	Loading event (Date)	Soffit and Web cast on 4/05/05	Deck cast on 5/3/05
5/20/2005	Prestressing (5/20/05)	5.59 (38.54)	3.99 (27.50)
7/25/2005	Removal of falsework (7/29/05)	5.13 (35.35)	5.45 (37.60)

Table 2.5 - Weighed-average concrete compressive strengths in ksi (MPa) for Frames 4 and 5

Loading event	Frame 4	Frame 5
Prestressing	5.56 (38.37)	5.08 (35.06)
Removal of formwork	5.78 (39.85)	5.23 (36.06)

The modulus of elasticity of the concrete was determined from the concrete compressive strengths according to the formula in ACI 209 and AASHTO 2004 (Kim 2009). The average values determined for Frames 4 and 5 based on the compressive strengths on the day of prestressing are 4,496 ksi (31 GPa) and 4,351 ksi (30 GPa), respectively.

2.2 I215-CA91 Northwest and Southeast Connectors

The northwest (NW) and southeast (SE) connectors on I215-CA91 are located in Riverside, California. Riverside has dry and hot summers and mild winters, and has a year-round average relative humidity of 34-37%. The NW connector has three frames, while the SE connector has six. The monitored girder segments are Span 2 (in Frame 1) of the NW connector and Span 16 (in Frame 5) of the SE Connector. The post-tensioned bridge girder has a trapezoidal cross-sectional shape with three cells. A typical girder section is shown in Fig. 2.5. The monitored sections are at midspan and near a bent. As shown in Fig. 2.6, Span 2 (in Frame 1) is 60 m long and Span 16 (in Frame 5) is 70 m.

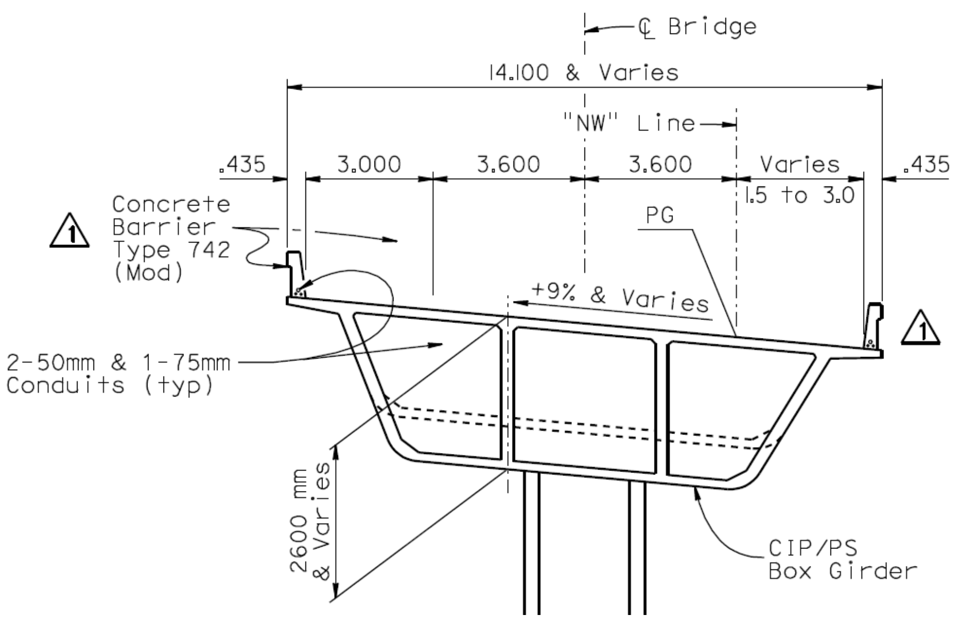

Fig. 2.5 – Typical girder cross section in I215-CA91 (Caltrans Design Drawings)

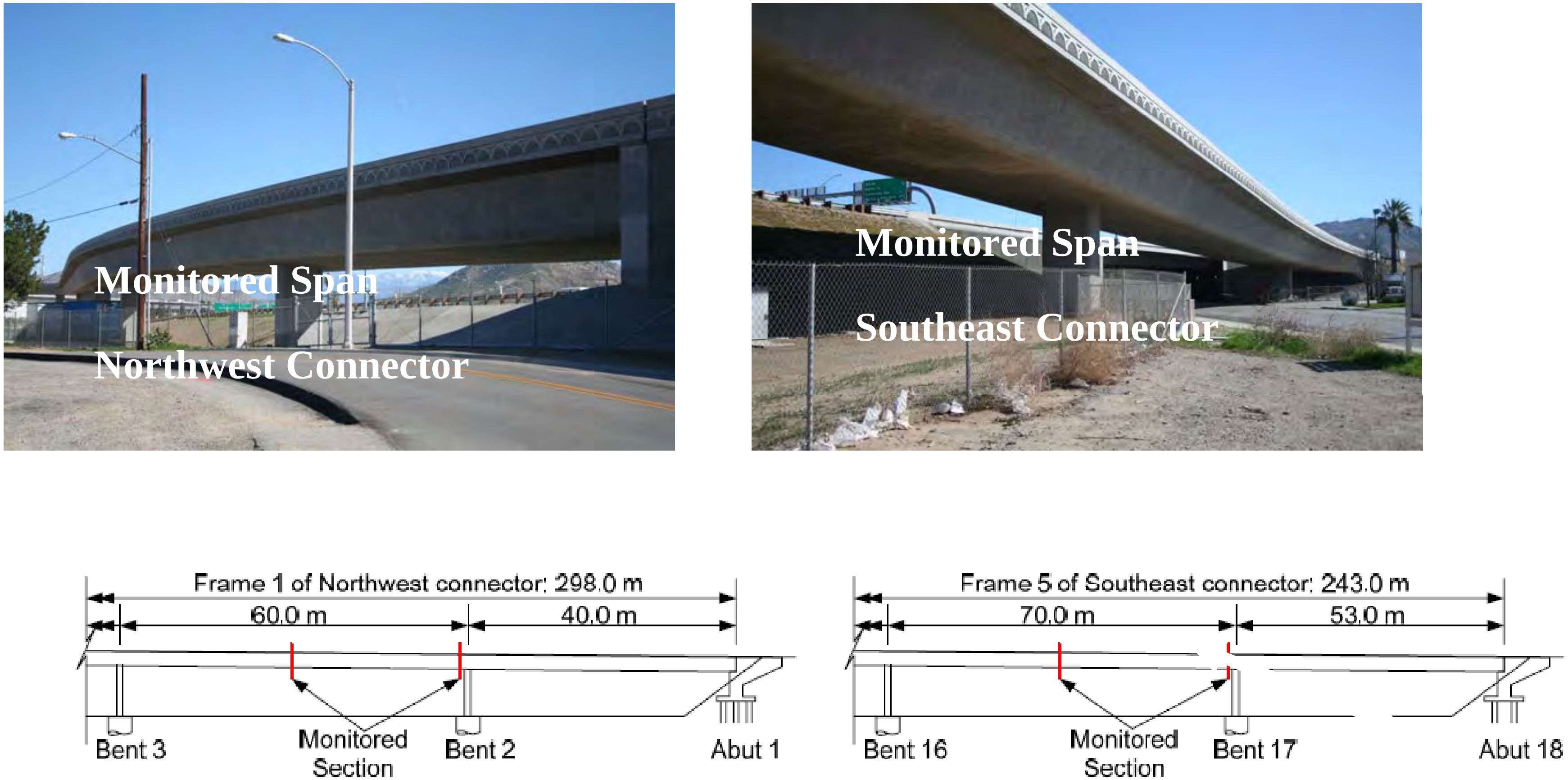

Fig. 2.6 – Bridge elevation view and monitored sections of I215-CA91 connectors (Kim 2009)

The soffit and webs of the NW connector girder were cast on February 2, 2006, and the deck on June 2, 2006. Prestressing occurred on June 30 of the same year, and the falsework was removed on September 15. The above dates are summarized in Table 2.6.

The SE connector girder was constructed in two stages. The soffit and webs were cast on August 3, 2006. The deck was poured on October 26, 2006. Prestressing took place on November 17, 2006, and the removal of falsework on February 15, 2007. These dates are summarized in Table 2.7.

Table 2.6 - Construction time log and age of concrete at loading event for NW connector

Loading event (Date)	Casting dates and concrete age (in days) at loading	
	Soffit and Web (2/2/06)	Deck (6/2/06)
Prestressing (6/30/06)	148	28
Removal of falsework (9/15/06)	225	105

Table 2.7 - Construction time log and age of concrete at loading event for SE connector

Loading event (Date)	Casting dates and concrete age (in days) at loading	
	Soffit and Web (8/3/06)	Deck (10/26/06)
Prestressing (11/17/06)	106	22
Removal of falsework (2/15/07)	196	112

The prestressing strand used in I215-CA91 is Grade 270 (1,860 MPa tensile strength) with a nominal yield strength of 230 ksi (1,586 MPa). The forces applied at the monitored sections, after immediate losses, are 9,483 kips (42,186 kN) at both the midspan and bent locations of the NW connector, and 9,368 kips (41,674 kN) and 9,359 kips (41,635 kN) at the respective sections of the SE connector girder.

The mild reinforcement used is Grade 60. At the monitored girder sections in the NW connector, the total cross-sectional area of the mild reinforcement is 25.56 in.^{2} (165 cm^2) in the top flange and 51.44 in.^{2} (332 cm^2) in the bottom flange. At the girder sections in the SE connector, the total mild reinforcement used is 28.92 in.^{2} (187 cm^2) in the top flange and 63.63 in.^{2} (411 cm^2) in the bottom flange. The elevation and cross-sectional views of the monitored girders are shown in Figs. 2.7 and 2.8. The cross-sectional areas of the girder in the NW connector are 10,602 in.^{2} (6.84 m^2) at midspan and 12,307 in.^{2} (7.94 m^2) at the section near the bent. For the girder in the SE connector, the respective areas are 12,028 in.^{2} (7.76 m^2) and 13,330 in.^{2} (8.60 m^2).

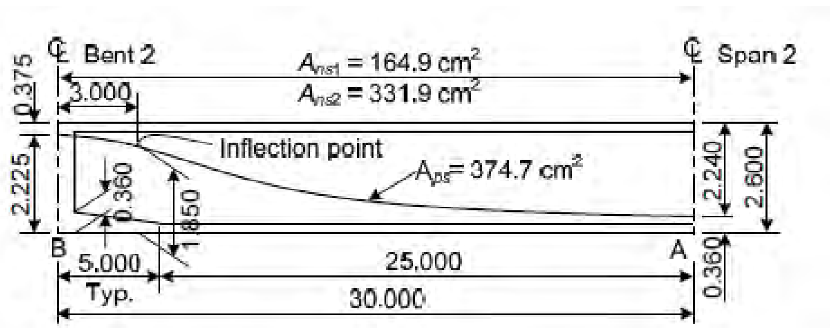

(a) Half elevation view

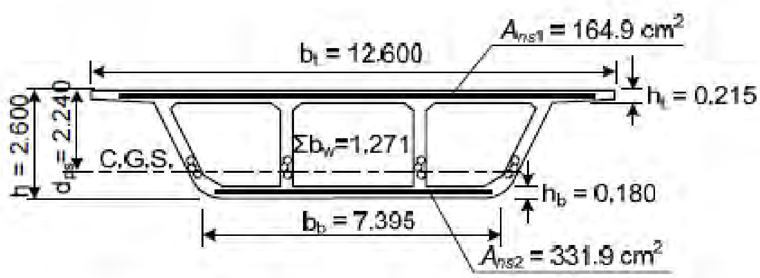

(b) Cross section at midspan

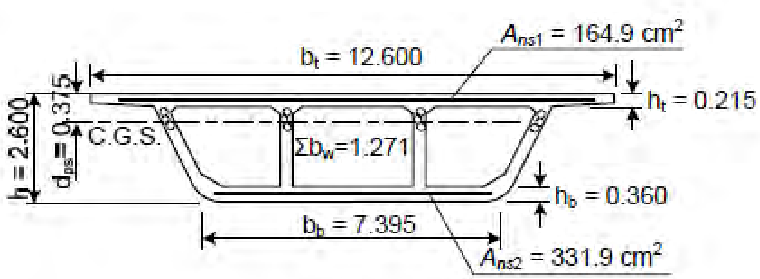

(c) Cross section near bent

Fig. 2.7 – Half elevation and cross-sectional views of girder in NW connector on I215-CA91 (Kim 2009)

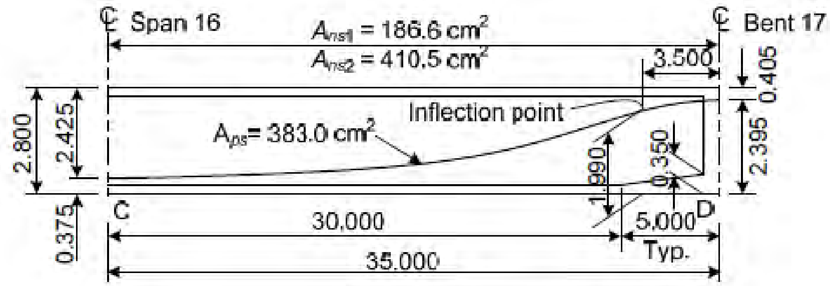

(a) Half elevation view

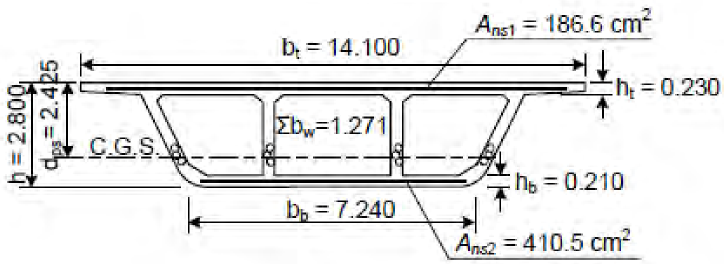

(b) Cross section at midspan

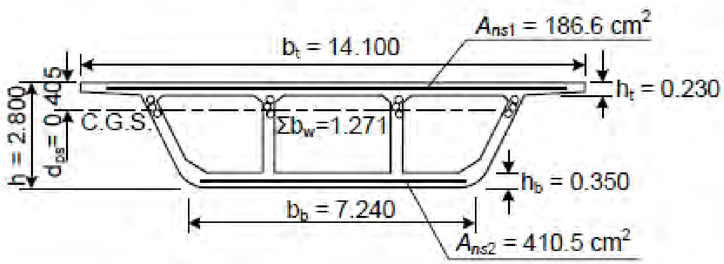

(c) Cross section near bent

Fig. 2.8 – Half elevation and cross-sectional view of the girder in SE connector on I215-CA91 (Kim 2009)

Material tests were conducted on concrete cylinders to determine the creep coefficients and shrinkage strains as a function of time. The concrete cylinders were cast with the same batches of concrete used in the bridge girders. A total of sixteen 12 x 6 in. (300 x 150 mm) cylinders were cast. The specimens were kept in a maintenance yard of the California Department of Transportations near the bridge site to be exposed to the same environmental conditions as the actual bridge. The procedures followed for the determination of the material properties are the same as those for the I5-I805 connector, which is described in Section 2.1.

The creep and shrinkage properties obtained will be presented in Section 3.3. The strength data obtained from the compression tests are summarized in Tables 2.8 and 2.9. The weighted-average compressive strengths (based on the proportions of the cross-sectional areas of the soffit and the deck) are shown in Table 2.10. Concrete strengths at 28 days are not available from the data base. As mentioned previously, using the compressive strength of concrete at the time of prestressing, which was longer than 28 days, in the AASHTO 2004 formula for creep could result in a slightly lower creep and prestress loss.

Table 2.8 - Test dates and compressive strengths in ksi (MPa) for NW connector

Test Date	Loading Event (Date)	Soffit and Web cast on 2/2/06	Deck cast on 6/2/06
6/30/2006	Prestressing (6/30/06)	6.75 (46.54)	4.97 (34.23)
9/28/2006	Removal of falsework (9/15/06)	6.88 (47.44)	4.95 (34.09)

Table 2.9 - Test dates and compressive strength in ksi (MPa) for SE connector

Test Date	Loading Event (Date)	Soffit and Web cast on 8/3/06	Deck cast on 10/26/06
11/17/2006	Prestressing (11/17/06)	5.58 (38.47)	5.24 (36.13)
2/23/2007	Removal of falsework (2/15/07)	5.86 (40.37)	5.79 (39.89)

Table 2.10 - Weighed-Average compressive strengths in ksi (MPa) for NW and SE connectors

Loading event	NW	SE
Prestressing	6.04 (41.65)	5.44 (37.54)
Removal of falsework	6.11 (42.13)	5.83 (40.22)

The modulus of elasticity of the concrete in the NW connector is 4,713 ksi (32.5 GPa), and that in the SE connector is 4,467 ksi (30.8 GPa). These values were estimated based on the concrete compressive strengths on the day of prestressing according to the formula given in ACI 209 and AASHTO 2004 (Kim 2009).

3 Creep and Shrinkage of Concrete

In this chapter, formulas adopted by the Third (2004) and Fourth (2007) Editions of the AASHTO LRFD Bridge Design Specifications for estimating the creep and shrinkage of concrete are summarized and compared to the material data obtained by Kim (2009) for the monitored bridges described in Chapter 2. The formulas in the AASHTO 2007 Specifications are different from those in the 2004 Spectifications and are based on the work of Tadros et al. (2003). In a project support by the National Cooperative Highway Research Program, Tadros et al. (2003) have studied the creep and shrinkage properties of twelve high-strength concrete mixes used by different suppliers in Nebraska, New Hampshire, Texas, and Washington for the construction of pretensioned bridge girders. The 28-day compressive strengths of the concrete based on these mix designs varied from 6.4 to 13.3 ksi, and most of the creep specimens used in their study were loaded at the age of one day. The specimens had a volume-to-surface area (*V*/*S*) ratio of 1 in. (25.4 mm) and were left to cure at an ambient room temperature of around 73^{o}F (23^{o}C). They have found that the AASHTO 2004 formulas tend to over-estimate the creep and shrinkage of the concrete specimens by a significant amount. Based on these results, they have proposed new formulas to provide a better correlation with their material data. In their formulas, the correction factor for the *V*/*S* ratio is assumed to be the same for both creep and shrinkage, and it is normalized so that it has a value of one when *V*/*S* is 3.5 inches. The expression for this factor is obtained from the original expression for shrinkage in the AASHTO 2004 Specifications by dropping the time-dependency term.

3.1 AASHTO 2004 Specifications

3.1.1 Shrinkage

According to the AASHTO 2004 LRFD Specifications, the shrinkage strain of moist-cured concrete is estimated with the following formula.

$$\varepsilon_{sh}(t) = k_{ss} k_{hs} k_{tds} \times 0.51 \times 10^{-3} \tag{3.1a}$$

where

$$k_{ss} = \left[\frac{\dfrac{t}{26e^{0.36(V/S)} + t}}{\dfrac{t}{45+t}} \right] \left[\frac{1064 - 94(V/S)}{923} \right] \tag{3.1b}$$

$$k_{hs} = \frac{140 - H}{70} \text{ for } H < 80\% \text{ and } \frac{3(100 - H)}{70} \text{ for } H \geq 80\% \tag{3.1c}$$

$$k_{tds} = \frac{t}{35 + t} \tag{3.1d}$$

with

t = days from end of curing

V / S = volume-to-surface area ratio (in.) with a maximum allowable value of 6 in.

H = relative humidity (%)

For poorly ventilated enclosed cells, only 50% of the interior perimeter should be used to calculate the surface area S.

3.1.2 Creep

According to AASHTO 2004, the creep coefficient is estimated with the following formula.

$$\psi(t, t_i) = 3.5 k_{sc} k_{hc} k_f k_{tdc} t_i^{-0.118} \tag{3.2a}$$

where

$$k_{sc} = \left[\frac{\dfrac{t - t_i}{26e^{0.36(V/S)} + (t - t_i)}}{\dfrac{(t - t_i)}{45 + (t - t_i)}} \right] \left[\frac{1.80 + 1.77e^{-0.54(V/S)}}{2.587} \right] \tag{3.2b}$$

$$k_{hc} = 1.58 - \frac{H}{120} \tag{3.2c}$$

$$k_f = \frac{1}{0.67 + \dfrac{f'_c}{9}} \tag{3.2d}$$

$$k_{tdc} = \frac{(t - t_i)^{0.6}}{10 + (t - t_i)^{0.6}} \tag{3.2e}$$

with

t = age of concrete (days)

t_i = age of concrete at time of prestressing or load application (days)

f_c' = compressive strength of concrete at 28 days (ksi)

3.2 AASHTO 2007 Specifications

Methods for calculating the creep and shrinkage of concrete are identical in the Fourth (2007) and Fifth (2010) Editions of the AASHTO LRFD Specifications. They are presented below.

3.2.1 Shrinkage

According to the AASHTO 2007 Specifications, the shrinkage of concrete is estimated with the following formula.

$$\varepsilon_{sh}(t) = k_s k_{hs} k_f k_{td} \times 0.48 \times 10^{-3} \tag{3.3a}$$

where

$$k_s = 1.45 - 0.13(V / S) \geq 1.0 \tag{3.3b}$$

$$k_{hs} = 2.00 - 0.014H \tag{3.3c}$$

$$k_f = \frac{5}{1 + f_{ci}'} \tag{3.3d}$$

$$k_{td} = \frac{t}{61 - 4 f_{ci}' + t} \tag{3.3e}$$

with

t = days from end of curing

V/S = volume-to-surface area ratio (in.)

H = relative humidity (%)

f'_{ci} = compressive strength of concrete at prestressing (ksi)

For poorly ventilated enclosed cells, only 50% of the interior perimeter should be used to calculate the surface area. As mentioned previously, Eq. (3.3b) is a simplification of Eq. (3.1b) by dropping the time-dependency term and having the correction factor so normalized that it assumes a value of one when *V/S* = 3.5 inches.

3.2.2 Creep

According to AASHTO 2007, the creep coefficient is estimated with the following formula.

$$\psi(t,t_i) = 1.9 k_s k_{hc} k_f k_{td} t_i^{-0.118} \tag{3.4a}$$

$$k_{hc} = 1.56 - 0.008H \tag{3.4b}$$

$$k_{td} = \frac{t - t_i}{61 - 4f'_{ci} + (t - t_i)} \tag{3.4c}$$

with

t = age of concrete (days)

t_i = age of concrete at time of prestressing or load application (days)

In the above expression, k_s is calculated with Eq. (3.3b).

3.3 Comparison of AASHTO Formulas with Measured Data

The AASHTO formulas are evaluated with the creep and shrinkage data obtained by Kim (2009) from 6-in.-x-12-in. (150-mm-x-300-mm) concrete cylinders prepared with concrete batches used to construct the monitored bridge girders. Except for Frame 4 of the I5-I805 connector, which was cast in three stages, all girders were cast in two stages starting from the soffit to the deck with months apart. The data considered here are from concrete specimens prepared during the first pour (soffit) for each girder. The specimens were air-cured under the same environment as the bridge girders and the creep specimens were loaded on the same day when post-tensioning took place. The strengths, curing conditions, and age of the concrete at post-tensioning are summarized in Table 3.1. The shrinkage data are plotted in Figs. 3.1 through 3.3, while the creep data are shown in Figs. 3.4 through 3.7. Some of the plots have less data points than the others because some data are deemed unreliable (showing large scatter), and are, therefore, discarded. The shrinkage strains obtained for Frame 4 are extremely high probably because the concrete cylinders were not exposed to an appropriate drying condition as noted by Kim (2009). Therefore, the shrinkage data for Frame 4 are deemed unreliable and are not shown here. As it will be discussed in Section 4.2.1, the shrinkage data on the May batch for Frame 5 will be used instead for the calculation of prestress losses for Frame 4.

Table 3.1 - Strengths and curing conditions of concrete

	I5-I805		I215-CA91	
Parameters	Frame 4	Frame 5	NW connector	SE connector
Cylinder *V/S*, in. (mm)	1.5 (38)	1.5 (38)	1.5 (38)	1.5 (38)
Girder *V/S*, in. (mm)	4.8 (122)	4.5 (114)	5.0 (127)	5.3 (134)
Average Relative Humidity, %	66	65	35	37
Compressive strength*, ksi (MPa)	5.94 (40.9)	5.59 (38.5)	6.75 (46.5)	5.58 (38.5)
Concrete age at end of curing, days	7	7	7	7
Concrete age at post-tensioning, days	175	45	148	106

*This is the strength measured soon after prestressing from concrete cylinders for the soffit; it is expected to be slightly higher than the 28-day strength

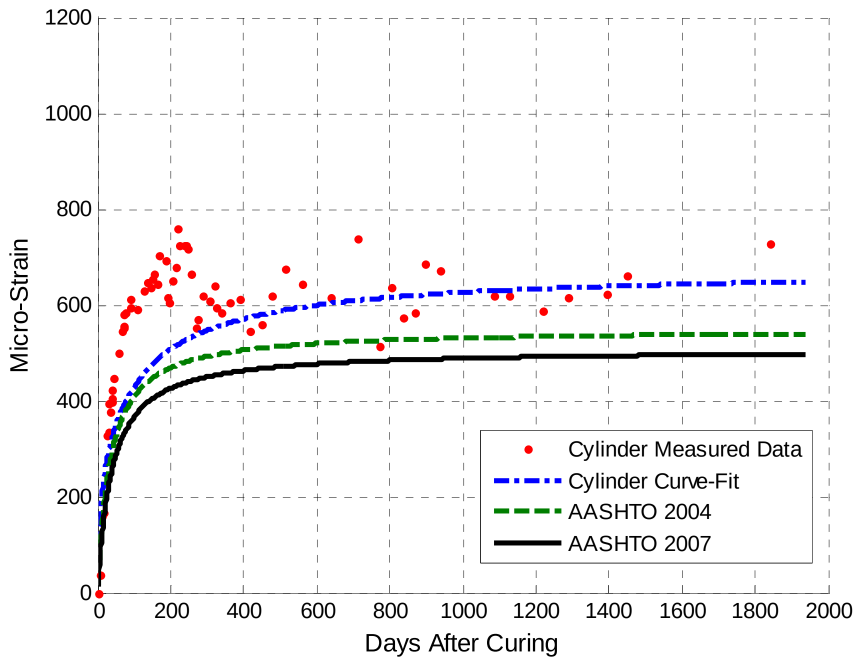

Fig. 3.1 - Shrinkage strain for April batch for Frame 5 of I5-I805 connector

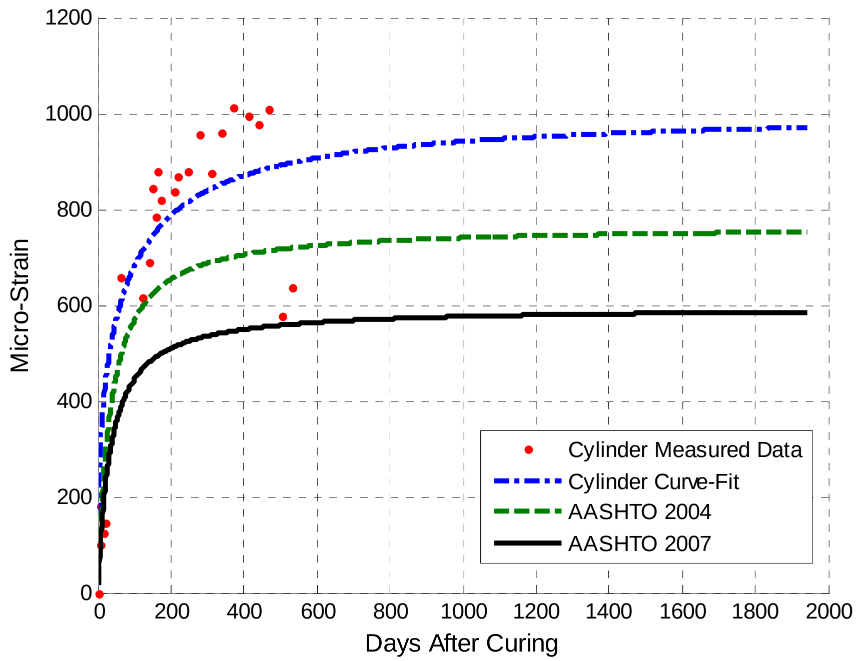

Fig. 3.2 – Shrinkage strain for February batch for NW connector of I215-CA91

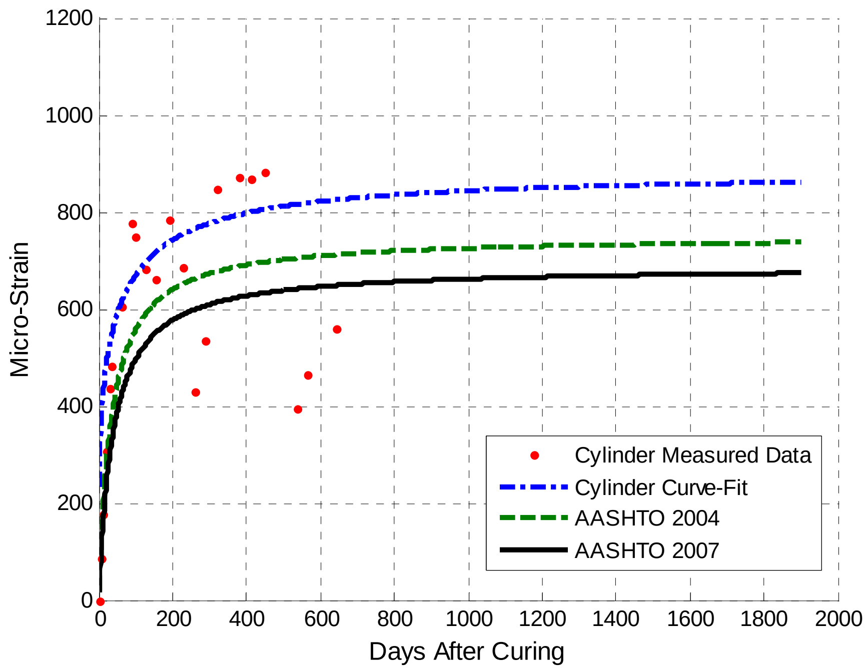

Fig. 3.3 - Shrinkage strain for August batch for SE connector of I215-CA91

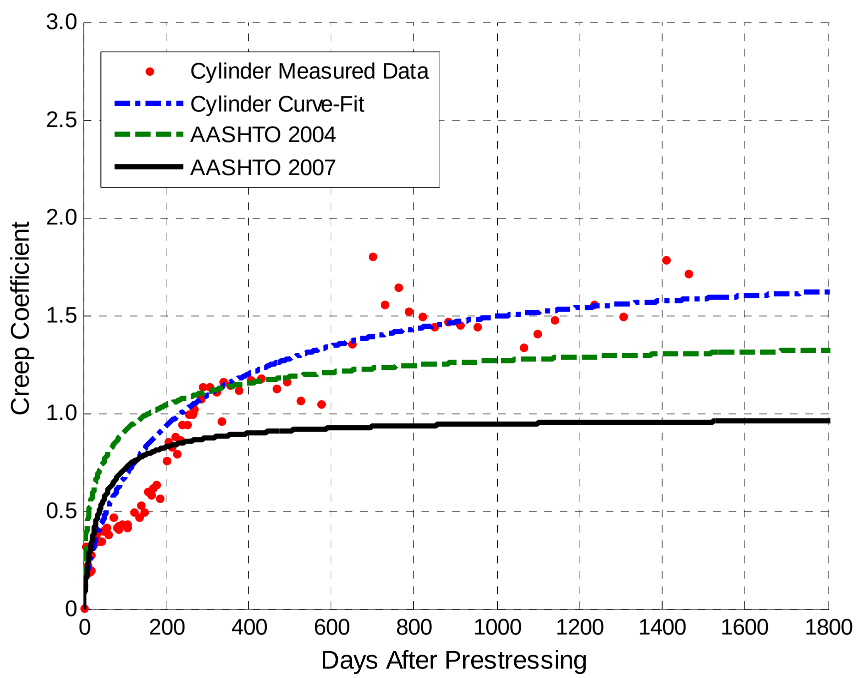

Fig. 3.4 - Creep coefficient for October batch for Frame 4 of I5-I805 connector

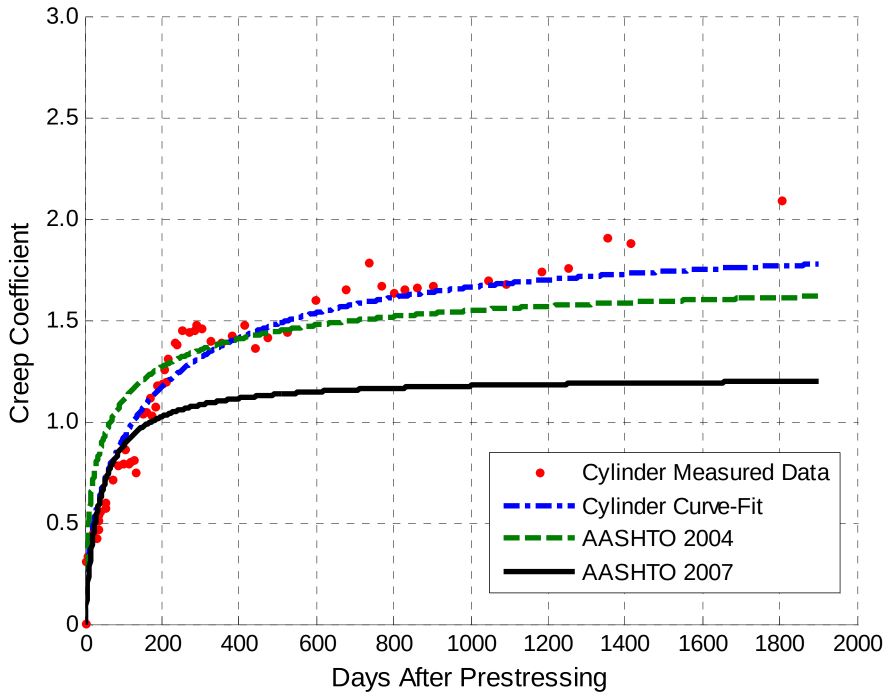

Fig. 3.5 - Creep coefficient for April batch for Frame 5 of I5-I805 connector

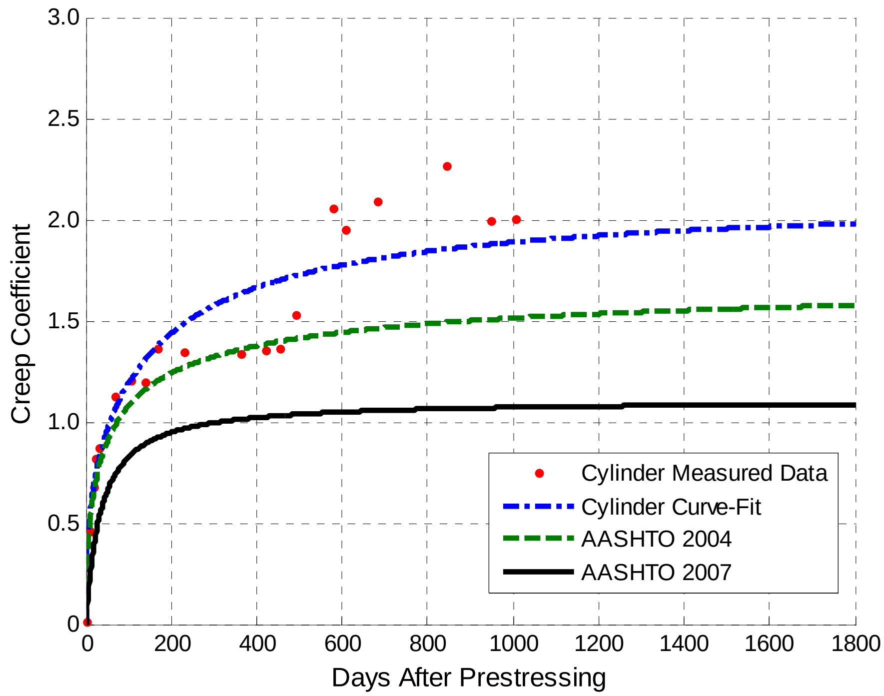

Fig. 3.6 - Creep coefficient for February batch for NW connector of I215-CA91

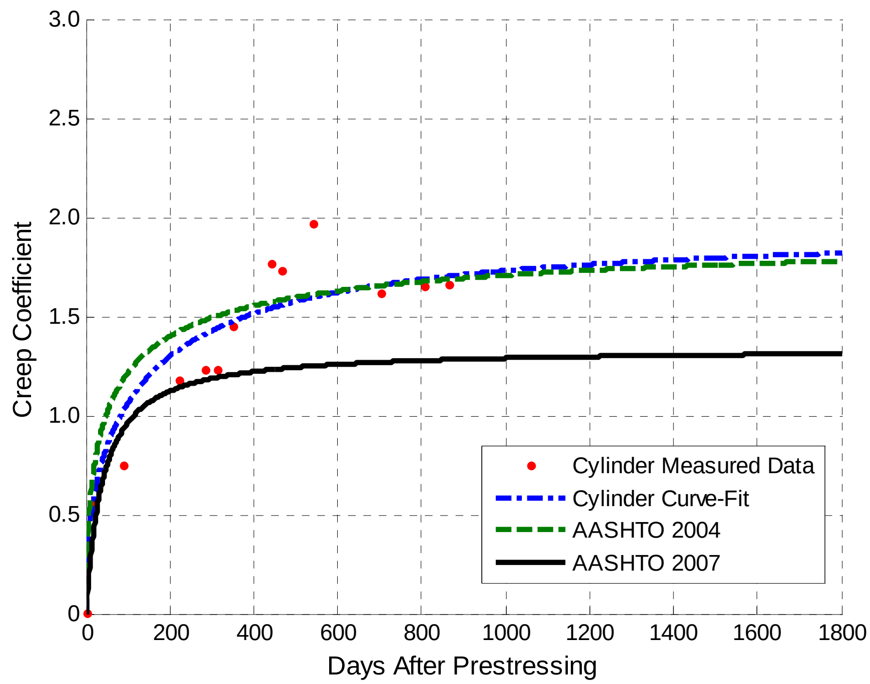

Fig. 3.7 - Creep coefficient for August batch for SE connector of I215-CA91

A best-fit curve is also obtained for the measured data and compared to the predictions obtained with the AASHTO formulas. The best-fit curve is obtained with a method used by Kim (2009). It can be observed from Figs. 3.1 through 3.7 that both the AASHTO 2004 and 2007 formulas under-predict the creep and shrinkage. However, the formulas in AASHTO 2004 provide a much better match.

The reason that the AASHTO 2007 Specifications give much lower creep and shrinkage values than the 2004 Specifications could be that the 2007 formulas were calibrated with data obtained from high-strength concrete that had compressive strengths ranging from 6,000 to 9,000 psi, with the majority of the strengths on the high side, while the concrete considered here had a strength around 6,000 psi or lower. Even though the compressive strength of concrete is taken into considerations in these formulas, the adopted relation may not be appropriate for lower-strength concrete.

4 Refined Analysis Methods

Different refined analysis methods have been developed to evaluate the immediate and long-term prestress losses in prestressed concrete members. This report focuses only on the long-term losses, which can be contributed by the creep and shrinkage of concrete as well as the relaxation of the prestressing steel. Hence, the total long-term prestress loss Δf_{pLT} consists of the following contributions.

$$\Delta f_{pLT} = \Delta f_{pC} + \Delta f_{pS} + \Delta f_{pR} \tag{4.1}$$

where Δf_{pC} is the creep loss, Δf_{pS} is the shrinkage loss, and Δf_{pR} is the relaxation loss. While a most refined approach to estimate these losses is to use the time-step analysis method, the required effort is often not warranted in view of the various uncertainties in the time-dependent behavior of the concrete and prestressing steel. The 2007 and 2010 Editions of the AASHTO LRFD Specifications have adopted a one-step refined analysis method as well as an approximate method to evaluate each of the above loss contributions. Both methods are based on the work of Tadros et al. (2003), which was focused on pretensioned bridge girders with high-strength concrete. Hence, these methods do not adequately account for the different conditions of post-tensioned members, which, for example, can have higher quantities of mild reinforcement than pretensioned members. Youakim and Karbhari (2006) have developed a refined analysis method for post-tensioned girders. This method is presented below and will be evaluated with the prestress loss data obtained from the monitored bridges that are described in Chapter 2. In addition, a new refined analysis method, which is similar in form to the current AASHTO method, is proposed here for post-tensioned girders, and it will be compared to the method of Youakim and Karbhari.

4.1 Youakim and Karbhari’s Method

The analysis method proposed by Youakim and Karbhari (2006) for calculating long-term prestress losses in post-tensioned girders is based on an approach that is described in Ghali et al. (2002). It is similar in concept to the refined analysis method adopted in the current AASHTO LRFD Specifications in that it uses an age-adjusted modulus of elasticity of concrete (Bazant 1972) to account for the interaction of the gradual prestress losses with the creep behavior of concrete over time. Nevertheless, the final formulations of the two methods are quite different. The method proposed by Youakim and Karbhari (2006) is summarized below without derivation. The detailed derivation can be found in their report.

4.1.1 Creep and Shrinkage Losses

In Youakim and Karbhari's method, the total creep and shrinkage loss between time instants t and t_i is given by the following equation.

$$\Delta f_{pC}(t,t_i) + \Delta f_{pS}(t,t_i) = E_p \left\{ k_A \varepsilon_{free}(t,t_i) - \bar{e}_p \left[k_I \phi_{free}(t,t_i) + k_h \varepsilon_{free}(t,t_i) / h \right] \right\} \quad (4.2)$$

where

E_p = modulus of elasticity of the prestressing steel

$\bar{e}_p$ = eccentricity of the prestressing force with respect to the centroid of the age-adjusted transformed girder section; positive when the prestressing force is below the centroid of the section

h = depth of girder

t_i = age of concrete at the time of post-tensioning

$$k_A = \frac{A_c}{\bar{A}_t}$$

$$k_I = \frac{I_c}{\bar{I}_t}$$

$$k_h = \frac{A_c \Delta y h}{\bar{I}_t}$$

with

Δy = distance of the centroid of the age-adjusted transformed girder section from that of the net concrete section; positive if the former is below the latter

A_c, I_c = cross-sectional area and moment of inertia of the net concrete section

$\bar{A}_t, \bar{I}_t$ = cross-sectional area and moment of inertia of the age-adjusted transformed girder section, which includes the prestressing steel and mild reinforcement, and the transformed section is based on the age-adjusted modulus of elasticity of concrete, $\bar{E}_c(t, t_i)$

The age-adjusted modulus of elasticity of concrete is defined as

$$\bar{E}_c(t, t_i) = \frac{E_{ci}}{1 + \chi\psi(t, t_i)} \tag{4.3}$$

where $E_{ci} = E_c(t_i)$, the modulus of elasticity of concrete at the time of post-tensioning, and χ is a time averaging factor, whose value is recommended by Youakim and Karbhari to be 0.8. In AASHTO 2007, the time averaging factor is assumed to be 0.7 for the refined analysis method. Since the difference between the two recommended values is very small, the value of 0.7 is adopted for all the prestress-loss calculations conducted in this study to be consistent with the AASHTO specifications.

The free strain and free curvature are computed with the following equations. It should be noted that curvature is considered positive when it is concave upward.

$$\varepsilon_{free}(t, t_i) = \psi(t, t_i)\left[\varepsilon_o(t_i) - \phi(t_i)\Delta y_1\right] + \varepsilon_{sh}(t, t_i) \tag{4.4}$$

$$\phi_{free}(t, t_0) = \psi(t, t_i)\phi(t_i) \tag{4.5}$$

where Δy_1 is the distance of the centroid of the net concrete section from that of the initial transformed girder section (positive if the former is below the latter), which is defined below. The value of Δy_1 is normally very small so that it can be assumed zero. The shrinkage strain is defined as $\varepsilon_{sh}(t, t_i) = \varepsilon_{sh}(t) - \varepsilon_{sh}(t_i)$. The instantaneous strain $\varepsilon_o(t_i)$ at the centroid of the initial transformed section of the girder and the instantaneous curvature $\phi(t_i)$ can be computed as

$$\varepsilon_o(t_i) = \frac{A_{ps} f_{pi}}{E_{ci} A_t} \tag{4.6}$$

$$\phi(t_i) = \frac{M_{total}}{E_{ci} I_t} \tag{4.7}$$

with

A_{ps} = total cross-sectional area of the prestressing steel

f_{pi} = initial stress in the prestressing steel right after post-tensioning

M_{total} = total moment at the girder section right after post-tensioning; it is usually the sum of the moments induced by the self-weight and the equivalent load of the prestressing force

A_t, I_t = cross-sectional area and moment of inertia of the initial transformed girder section, which includes the net concrete section and mild reinforcement but excludes the prestressing steel; the transformed section is based on the elastic modulus of concrete, E_{ci}, at the time of post-tensioning

To separate the respective contributions of creep and shrinkage, Eq. (4.2) can be divided into the following two expressions with Δy_1 assumed to be zero.

$$\Delta f_{pC}(t,t_i) = E_p \psi(t,t_i)\left\{k_A \varepsilon_o(t_i) - \bar{e}_p\left[k_I \phi(t_i) + k_h \varepsilon_o(t_i)/h\right]\right\} \tag{4.8}$$

$$\Delta f_{pS}(t,t_i) = E_p\left\{k_A \varepsilon_{sh}(t,t_i) - \bar{e}_p\left[k_h \varepsilon_{sh}(t,t_i)/h\right]\right\} \tag{4.9}$$

4.1.2 Relaxation Loss

Based on a similar concept used by Tadros et al. (2003), Youakim and Karbhari (2006) have derived the following expression to calculate the relaxation loss of the prestressing steel.

$$\Delta f_{pR}(t,t_i) = \chi_r \Delta \tilde{f}_{pR}(t,t_i)\left[1 - \frac{E_p}{\bar{E}_c(t,t_i)}(k_{Ap} + k_y)\right] \tag{4.10}$$

with the value of χ_r recommended to be 0.7, which is to account for the influence of the creep and shrinkage losses on steel relaxation, and

$$k_{Ap} = \frac{A_{ps}}{\bar{A}_t} \tag{4.11}$$

$$k_y = \frac{A_{ps}\bar{e}_p^2}{\bar{I}_t} \tag{4.12}$$

$$\Delta\tilde{f}_{pR}(t,t_i) = \frac{\log(24(t-t_i))}{K'}\left(\frac{f_{pi}}{f_{py}} - 0.55\right) f_{pi} \tag{4.13}$$

where f_{py} is the yield strength of the prestressing steel and f_{pi} is the initial prestress in the steel. Equation (4.13) is a widely adopted empirical formula that was proposed by Magura et al. (1964) to estimate relaxation loss in prestressing strands subjected to a constant tensile strain. In the above expression, time is in days and t_i is the time at which the post-tensioning force is first applied. Youakim and Karbhari have suggested that K' be 40 for low-relaxation strands. However, in this study, K' is taken to be 45 for low-relaxation strands and 10 for other strands to be consistent with what that have been adopted in the AASHTO Specifications. In general, with low-relaxation strands, the contribution of steel relaxation to the total loss is relatively very small.

In lieu of the detailed calculation method shown above, Youakim and Karbhari (2006) have suggested the following simplification based on the properties of typical post-tensioned bridge girders that were identified in their survey. The bridges surveyed were either under construction or were soon to be constructed in California.

$$\Delta f_{pR}(t,t_i) = 0.85\chi_r \Delta\tilde{f}_{pR}(t,t_i) \tag{4.14}$$

4.2 Evaluation of Youakim and Karbhari's Method with Acquired Bridge Data

The refined analysis method of Youakim and Karbhari (2006) is evaluated with the prestress loss data acquired from the I5-I805 and I215-CA91 bridges, which are described in Chapter 2 of this report. For the loss calculations using the refined method, three sets of creep and shrinkage properties of concrete are considered. One is the material data obtained from concrete cylinders cast with the bridge girders. For this purpose, the best-fit curves for the cylinder data, as presented in Section 3.3, are adjusted to take into account the different *V*/*S* ratios of the bridge girders and the cylinders. These adjustments are made by using the formulas for the *V*/*S* correction factors in the 2004 AASHTO Specifications (i.e., Eq. (3.1b) and Eq. (3.2b) in the report) and the *V*/*S* ratios of the concrete cylinders and the girders presented in Table 3.1. In addition, long-term losses are also calculated using the creep and shrinkage formulas provided in the 2004 and 2007 AASHTO Specifications. The results are presented below.

4.2.1 I5-I805 Connector

The material and geometric properties, and other information for the girder sections on the I5-I805 connector used for the prestress-loss calculations are summarized in Table 4.1. The design and construction details of the bridge structures are described in Section 2.1.

Table 4.1 - Girder properties for I5-I805

Input Parameters	Frame 4		Frame 5	
	Midspan	Bent	Midspan	Bent
Girder cross-sectional area, in.^{2} (m^2)	12,617 (8.14)	16,926 (10.92)	10,881 (7.02)	13,423 (8.66)
Concrete Young's modulus, ksi (GPa)	4,525 (31.20)	4,525 (31.20)	4,322 (29.80)	4,322 (29.80)
Volume-to-surface ratio, *V*/*S*, in. (mm)	4.81 (122)	4.81 (122)	5.65 (144)	5.65 (144)
Age coefficient, χ	0.70	0.70	0.70	0.70
Concrete age at end of curing, days	7	7	7	7
Concrete age at prestressing, days	175	175	45	45
Mild reinforcement Young's modulus, ksi (GPa)	29,000 (200)	29,000 (200)	29,000 (200)	29,000 (200)
Prestressing steel Young's modulus, ksi (GPa)	28,000 (193)	28,000 (193)	28,000 (193)	28,000 (193)
Area of prestressing steel, in.^{2} (cm^2)	65.53 (422.8)	65.53 (422.8)	42.47 (274.0)	42.47 (274.0)
Distance of prestressing steel from top surface, in. (m)	110 (2.80)	16.9 (0.43)	76.4 (1.94)	13.4 (0.34)
Prestressing force, kips (kN)	11,653 (51,835)	11,720 (52,131)	7,563 (33,641)	7,878 (35,041)
Moment (due to self-weight & prestressing), kip-in (kN-m)	62,578 (7,071)	-269,961 (-30,503)	-2,276 (-257)	-44,933 (-5,077)
Relative humidity, %	66	66	65	65
Concrete strength at prestressing*, ksi (MPa)	5.94 (40.9)	5.94 (40.9)	5.59 (38.5)	5.59 (38.5)
Top mild reinforcement area, in.^{2} (cm^2)	56.4 (364)	56.4 (364)	56.4 (364)	56.4 (364)
Bottom mild reinforcement area, in.^{2} (cm^2)	48.2 (311)	48.2 (311)	48.2 (311)	48.2 (311)
Girder cross-sectional area, in.^{2} (m^2)	12,617 (8.14)	16,926 (10.92)	10,881 (7.02)	13,423 (8.66)
Distance of centroidal axis of concrete section from top surface, in. (m)	57.6 (1.46)	69.8 (1.77)	40.3 (1.02)	45.0 (1.14)
Span length, in. (m)	3,174 (80.6)		2,080 (52.8)	

*Assume that the concrete strengths at 28 days remain the same.

Calculated Losses for Frame 4

The three sets of shrinkage and creep properties of the girder concrete for Frame 4 used in the loss calculations are shown in Figs. 4.1 and 4.2. The curves with the “Bridge Curve-fit” label are derived from the cylinder best-fit curves based on the respective *V/S* factors for the cylinders and the girder. It should be noted that the shrinkage data acquired for this frame are not reliable due to an improper drying condition for the cylinders. For this reason, data from the May batch for Frame 5 are used instead as suggested by Kim (2009).

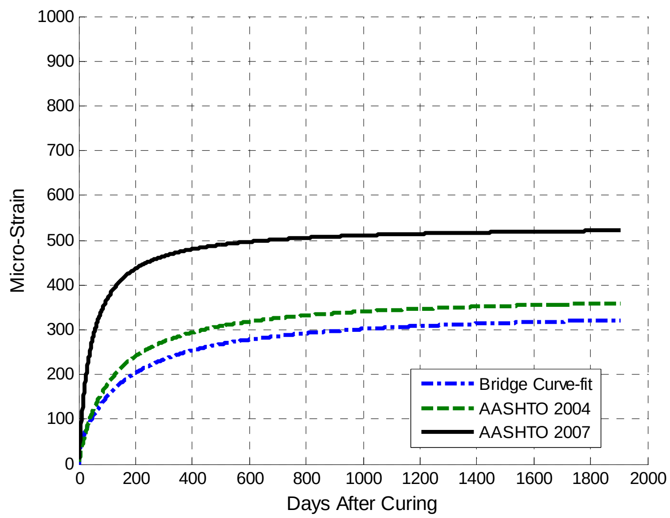

Fig. 4.1 – Girder shrinkage strain for May batch for Frame 5 of I5-I805 (used for Frame 4)

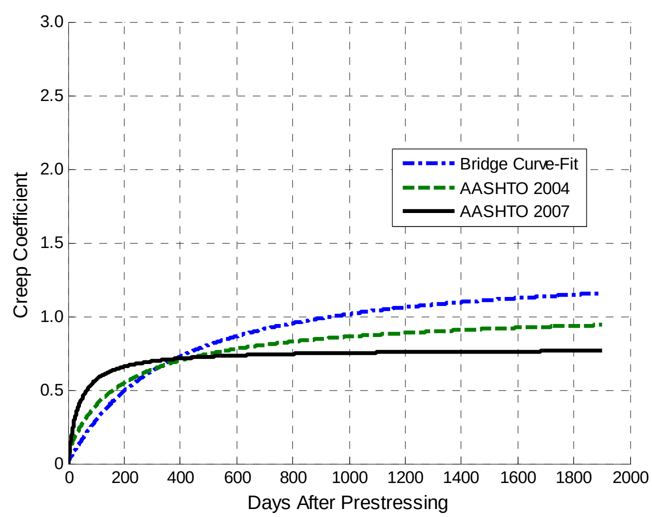

Fig. 4.2 - Girder creep coefficient for October batch for Frame 4 of I5-I805

For the two monitored girder sections in Frame 4, the time-dependent losses calculated with the refined method using the three sets of creep and shrinkage properties are compared to the measured losses in Figs. 4.3 and 4.4. The measured data show two time gaps with no data points. The first gap, between 520 and 680 days, is due to an unexpected incident in the data logging system. The second gap is due to the overwriting of data in the electronic file as data had not been downloaded for a while. Similar incidents occurred in the data sets for the other girder sections. The measured losses show cyclic changes with time. This is caused by the seasonal temperature variations that affected the prestressing forces. It can be observed that the losses calculated with the creep and shrinkage properties given in the AASHTO 2004 Specifications are close to those calculated with the measured material properties. In both cases, the calculated losses tend to be lower than the measured values, with the measured material properties providing a better correlation. For both the midpsan and bent locations, the discrepancy between the calculated and measured values is within a reasonable range. However, the losses calculated with the creep and shrinkage properties given in the AASHTO 2007 Specifications are a bit too low.

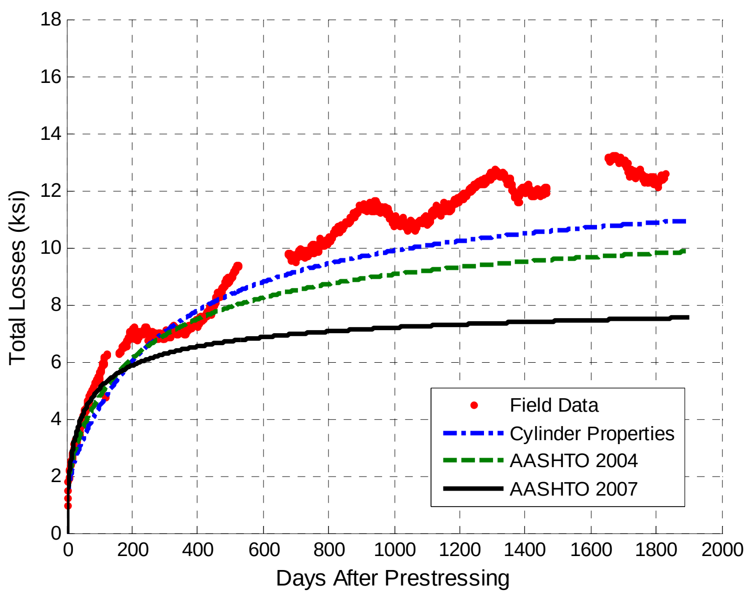

Fig. 4.3 – Total long-term prestress loss calculated with Youakim and Karbhari's method for midspan of Frame 4 of I5-I805

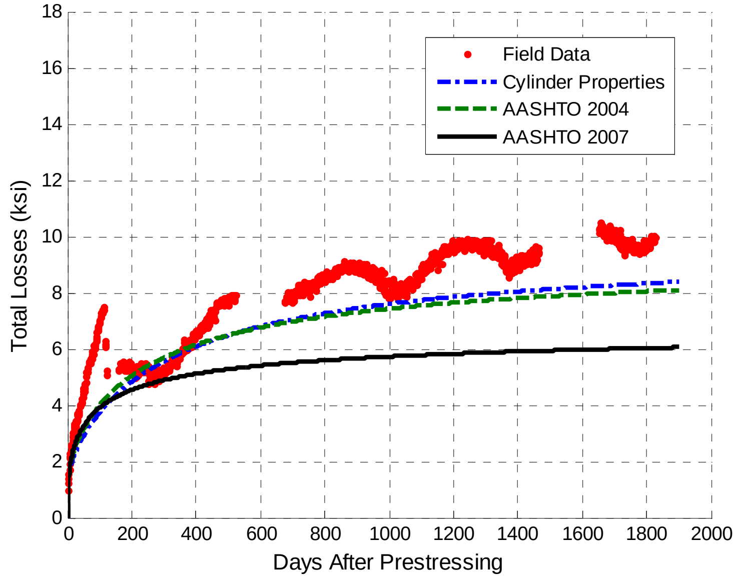

Fig. 4.4 – Total long-term prestress loss calculated with Youakim and Karbhari's method for section close to a bent of Frame 4 of I5-I805

Calculated Losses for Frame 5

The shrinkage and creep properties of the girder concrete for Frame 5 used in the loss calculations are shown in Figs. 4.5 and 4.6.

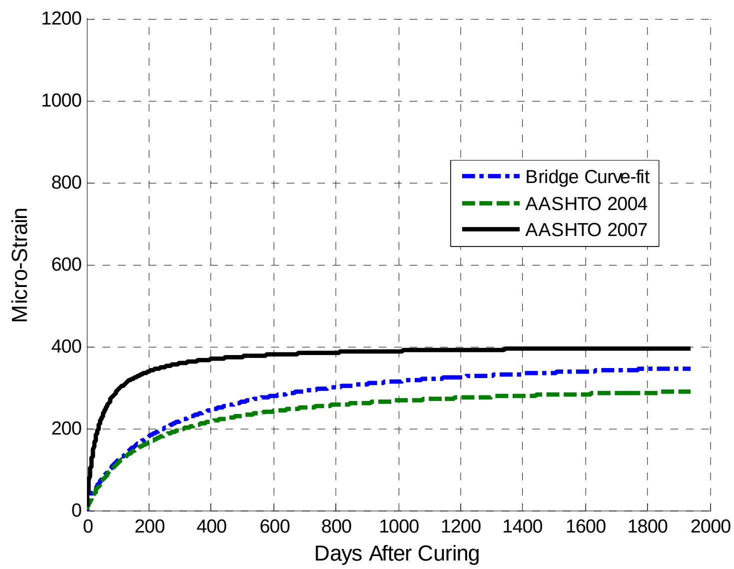

Fig. 4.5 - Girder shrinkage strain for April batch for Frame 5 of I5-I805 connector

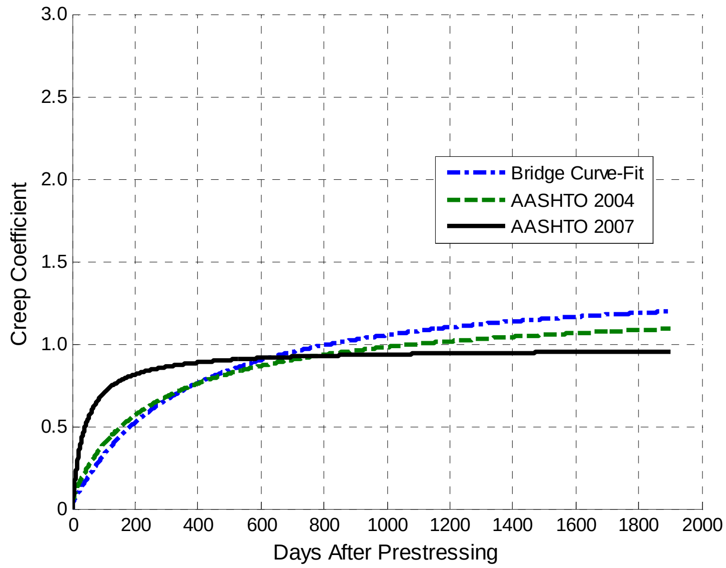

Fig. 4.6 - Girder creep coefficient for April batch for Frame 5 of I5-I805 connector

For the two monitored girder sections in Frame 5, the time-dependent losses calculated with the refined method using the three sets of creep and shrinkage properties are compared to the measured losses in Figs. 4.7 and 4.8. As shown, the losses calculated with the creep and shrinkage properties given in the AASHTO 2004 Specifications are a little lower than the values calculated with the measured material properties, with the latter a little closer to the measured losses. The losses calculated with the creep and shrinkage properties given in the AASHTO 2007 Specifications are a little lower than those with the AASHTO 2004 Specifications. The difference between the two is not as large as that for Frame 4.

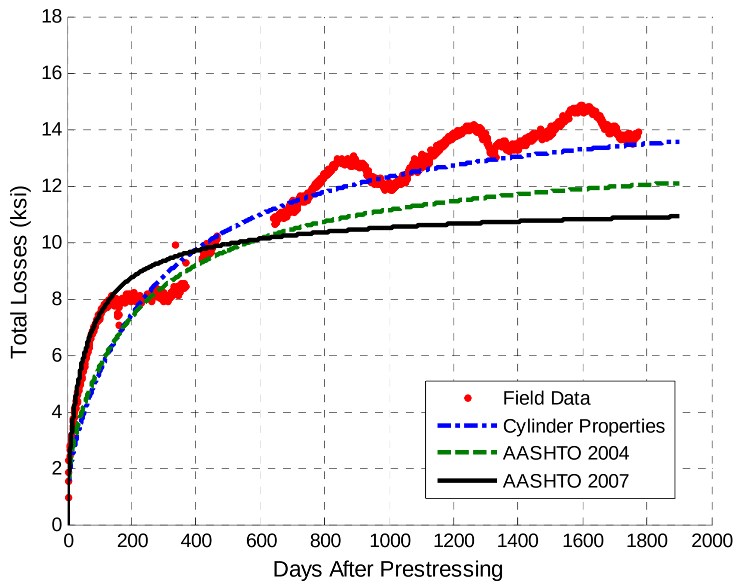

Fig. 4.7 – Total long-term prestress loss calculated with Youakim and Karbhari's method for midspan of Frame 5 of I5-I805

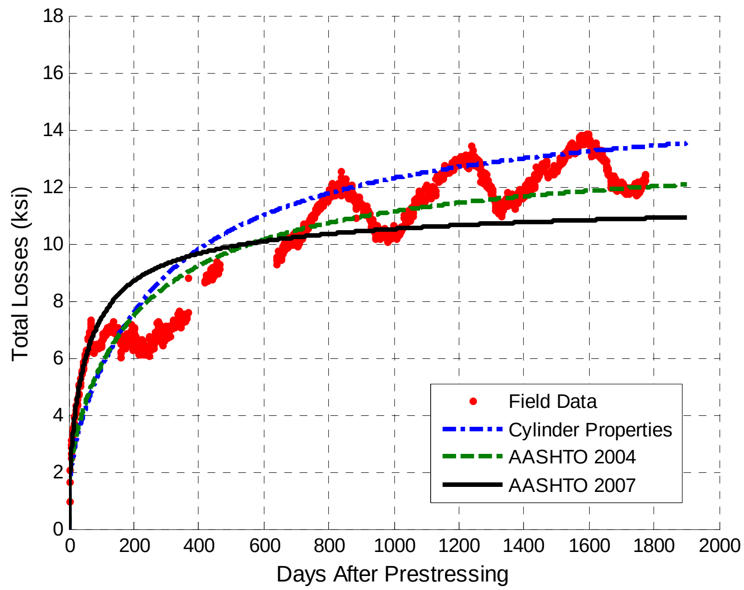

Fig. 4.8 – Total long-term prestress loss calculated with Youakim and Karbhari's method for section close to a bent of Frame 5 of I5-I805

The long-term losses at 1,800 days after prestressing calculated with the three sets concrete properties are compared to the measured values in Table 4.2. It can be seen that the refined method of Youakim and Karbhari provides reasonably good results with a discrepancy of 16% for the worst case when the measured material properties are used. The discrepancy is a little larger (23%) when the AASHTO 2004 Specifications for creep and shrinkage are used. The discrepancy is very significant (41%) when the AASHTO 2007 Specifications for creep and shrinkage are used. Except for one case, the calculated losses are lower than the measured values.

Table 4.2 - Prestress losses in I5-I805 bridge at 1800 days after prestressing

Method/Material Properties	Prestress Loss, ksi (MPa)			
	Frame 4		Frame 5	
	Midspan	Bent	Midspan	Bent
Measured	12.8 (88)	9.8 (68)	14.2 (98)	12.8 (88)
Calculated/Cylinder	10.9 (75) (-15%)	8.3 (57) (-16%)	13.5 (93) (-5%)	13.5 (93) (6%)
Calculated /AASHTO 2004	9.8 (68) (-23%)	8.1 (56) (-18%)	12.0 (83) (-15%)	12.0 (83) (-6%)
Calculated /AASHTO 2007	7.5 (52) (-41%)	6.1 (42) (-38%)	10.9 (75) (-24%)	10.9 (75) (-15%)

4.2.2 I215-CA91 Connectors

The material and geometric properties, and other information for the girder sections on the I215-CA91 connectors used for the prestress-loss calculations are summarized in Table 4.3. The design and construction details are described in Section 2.2.

Table 4.3 - Girder properties for I215-CA 91

Input Parameters	NW		SE	
	Midspan	Bent	Midspan	Bent
Girder cross-sectional area, in.^{2} (m^2)	10,602 (6.84)	12,307 (7.94)	12,028 (7.76)	13,330 (8.60)
Concrete Young's modulus, ksi (GPa)	4,713 (32.50)	4,713 (32.50)	4,467 (30.80)	4,467 (30.80)
Volume-to-surface ratio, *V/S*, in. (mm)	5.00 (127)	5.00 (127)	5.29 (134)	5.29 (134)
Age coefficient, χ	0.70	0.70	0.70	0.70
Concrete age at end of curing, days	7	7	7	7
Concrete age at prestressing, days	148	148	106	106
Mild reinforcement Young's modulus, ksi (GPa)	29,000 (200)	29,000 (200)	29,000 (200)	29,000 (200)
Prestressing steel Young's modulus, ksi (GPa)	28,000 (193)	28,000 (193)	28,000 (193)	28,000 (193)
Area of prestressing steel, in.^{2} (cm^2)	58.1 (375)	58.1 (375)	59.4 (383)	59.4 (383)
Distance of prestressing steel from top surface, in. (m)	88.2 (2.24)	15.0 (0.38)	95.5 (2.43)	15.9 (0.41)
Prestressing force, kips (kN)	9,484 (42,186)	9,484 (42,186)	9,369 (41,674)	9,360 (41,635)
Moment (due to self-weight & prestressing), kip-in (kN-m)	-50,990 (-5,761)	3,082 (348)	63,433 (7,167)	-196,370 (-22,188)
Relative humidity, %	35	35	37	37
Concrete strength at prestressing*, ksi (MPa)	6.75 (46.5)	6.75 (46.5)	5.58 (38.5)	5.58 (38.5)
Top mild reinforcement, in.^{2} (cm^2)	25.6 (165)	25.6 (165)	28.9 (187)	28.9 (187)
Bottom mild reinforcement, in.^{2} (cm^2)	51.4 (332)	51.4 (332)	63.6 (411)	63.6 (411)
Girder cross-sectional area, in.^{2} (m^2)	10,602 (6.84)	12,307 (7.94)	12,028 (7.76)	13,330 (8.60)
Distance of centroidal axis of concrete section from top surface, in. (m)	42.1 (1.07)	49.0 (1.25)	44.1 (1.12)	49.5 (1.26)
Span length, in. (m)	2,362 (60.0)		2,756 (70.0)	

* Assume that the concrete strengths at 28 days remain the same.

Calculated Losses for NW Connector

The shrinkage and creep properties of the girder concrete for the NW connector used in the loss calculations are shown in Figs. 4.9 and 4.10.

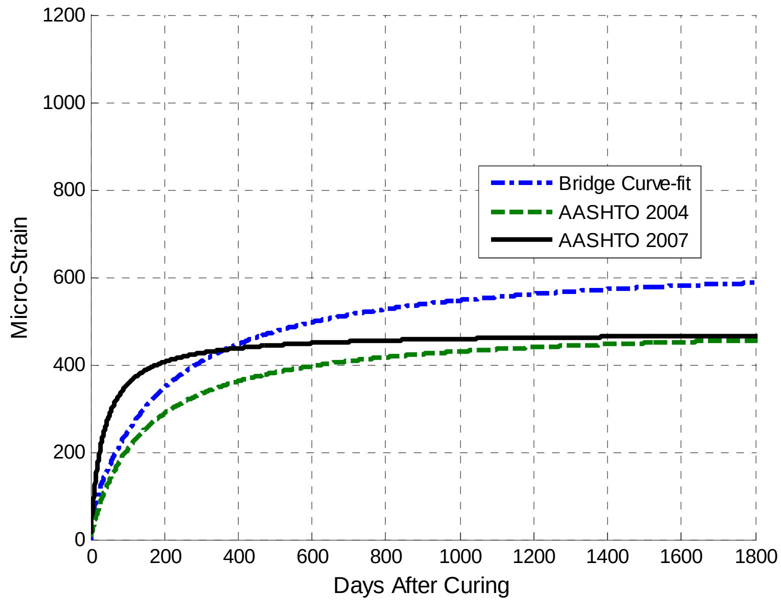

Fig. 4.9 - Girder shrinkage strain for February batch for NW connector of I215-CA91

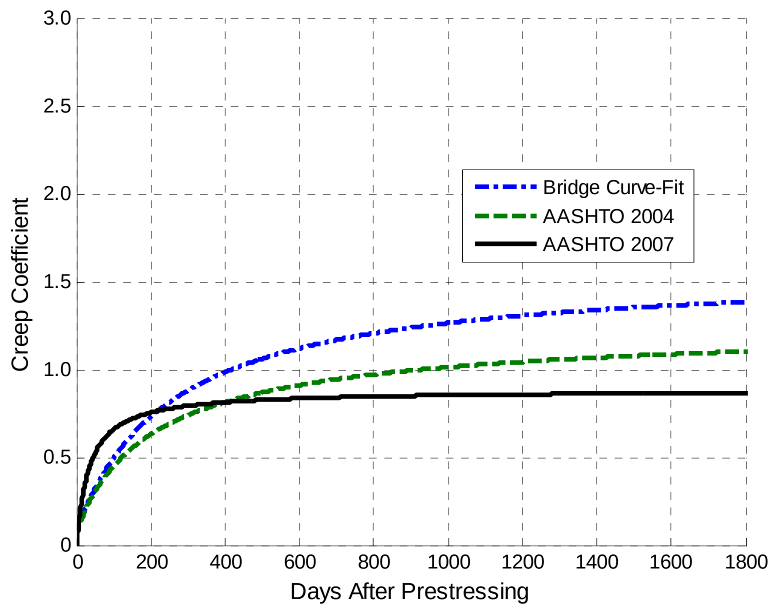

Fig. 4.10 - Girder creep coefficient for February batch for NW connector of I215-CA91

The time-dependent losses calculated with the refined method using the three sets of creep and shrinkage properties for the two monitored girder sections in the NW connector are compared to the measured loss data in Figs. 4.11 and 4.12. As shown, the losses calculated with the creep and shrinkage properties given in the AASHTO 2004 Specifications are a bit lower than those calculated with the measured material properties. The latter is closer to the loss measured at the midspan. However, for the section near a bent, the former slightly under-predicts and the latter slightly over-predicts the measured loss. The losses calculated with the creep and shrinkage properties given in the AASHTO 2007 Specifications are significantly lower than those with the AASHTO 2004 Specifications and the measured losses.

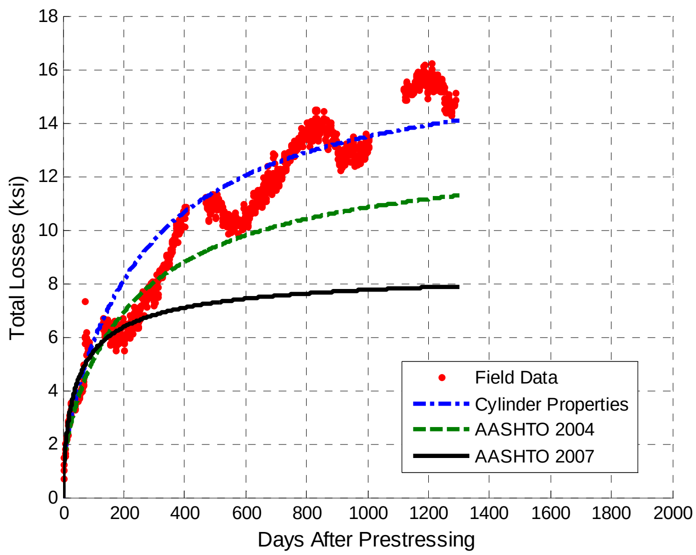

Fig. 4.11 – Total long-term prestress loss calculated with Youakim and Karbhari's method for midspan of NW connector of I215-CA91

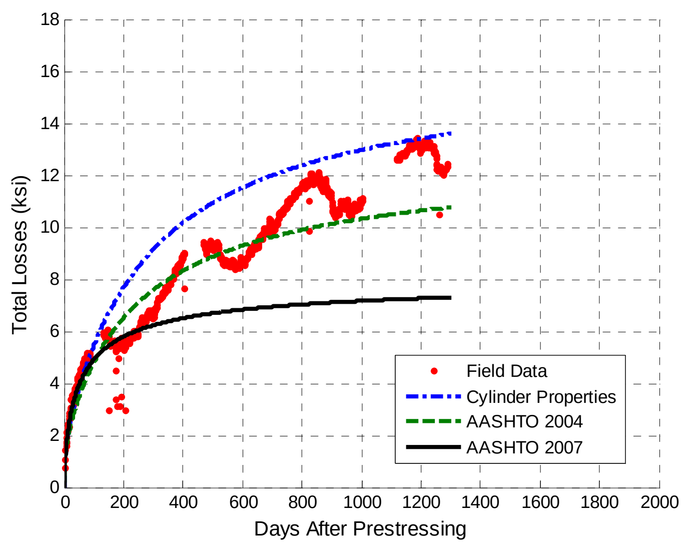

Fig. 4.12 – Total long-term prestress loss calculated with Youakim and Karbhari's method for section close to a bent of NW connector of I215-CA91

Calculated Losses for SE Connector

The shrinkage and creep properties of the girder concrete for the SE connector used in the loss calculations are shown in Figs. 4.13 and 4.14.

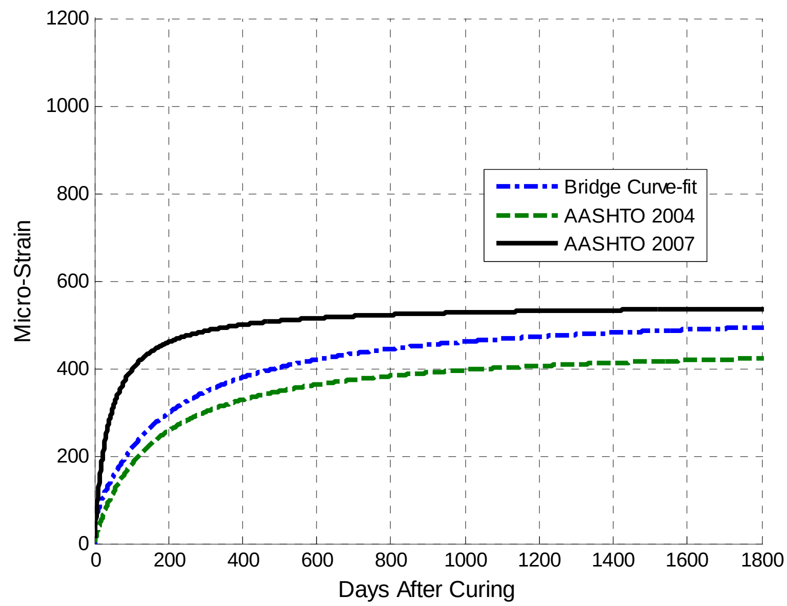

Fig. 4.13 - Girder shrinkage strain for August batch for SE connector of I215-CA91

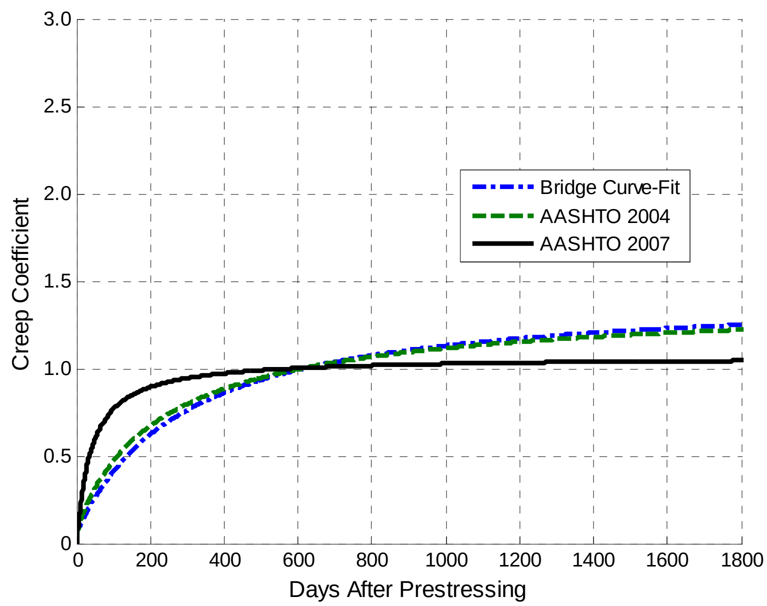

Fig. 4.14 - Girder creep coefficient for August batch for SE connector of I215-CA91

The time-dependent losses calculated with the refined method using the three sets of creep and shrinkage properties for the two monitored girder sections in the SE connector are compared to the measured values in Figs. 4.15 and 4.16. As shown, the losses obtained with the AASHTO 2004 Specifications for creep and shrinkage are a little lower than those calculated with the measure material properties. For the midspan section, both are very close to the measured losses. Nevertheless, for the section near a bent, the measured loss appears to be much lower than the calculated values. The very low measured loss at this section is difficult to explain. As in all other cases, the losses calculated with the AASHTO 2007 Specifications for creep and shrinkage are a lot lower than those with the AASHTO 2004 Specifications.

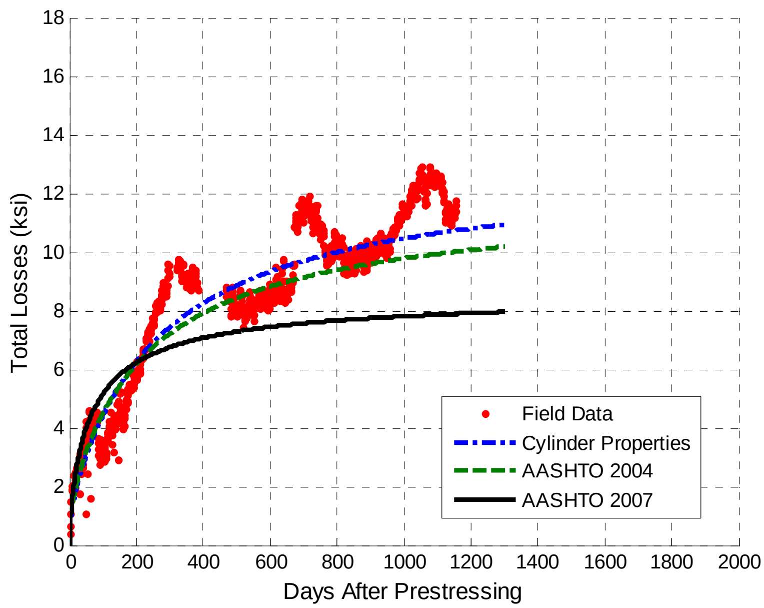

Fig. 4.15 – Total long-term prestress loss calculated with Youakim and Karbhari's method for midspan of SE connector of I215-CA91

The long-term losses at 1,200 days after prestressing calculated with the three sets of concrete properties are compared to the measured values in Table 4.4. In general, the refined analysis method gives satisfactory results except for the section near a bent in the SE connector, which has a very low measured loss. Except for this section, the discrepancy is 11% for the worst case when the measured material properties are used, while the maximum discrepancy is 27% when the AASHTO 2004 Specifications for creep and shrinkage are used in the calculations. The maximum discrepancy is 49% when the AASHTO 2007 Specifications for creep and shrinkage are used.

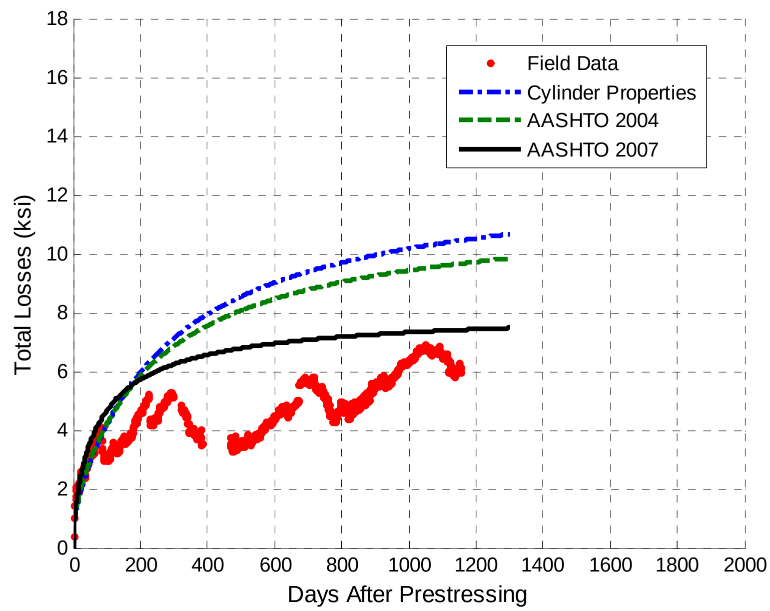

Fig. 4.16 – Total long-term prestress loss calculated with Youakim and Karbhari's method for section close to a bent of SE connector of I215-CA91

Table 4.4 - Prestress losses in I215-CA91 bridge at 1200 days after prestressing

Method/Material Properties	Prestress Loss, ksi (MPa)			
	NW Connector		SE Connector	
	Midspan	Bent	Midspan	Bent
Measured	15.2 (105)	12.5 (86)	12.2 (84)	6.5 (45)
Calculated/Cylinder	13.9 (96) (-9%)	13.5 (93) (8%)	10.9 (75) (-11%)	10.6 (73) (62%)
Calculated/AASHTO 2004	11.2 (77) (-27%)	10.6 (73) (-15%)	10.0 (69) (-18%)	9.7 (67) (49%)
Calculated/AASHTO 2007	7.8 (54) (-49%)	7.3 (50) (-42%)	8.0 (55) (-35%)	7.4 (51) (13%)

4.2.3 General Remarks

Since the AASHTO 2007 Specifications give lower creep and shrinkage values than the 2004 Specifications, the former will lead to lower long-term prestress losses as demonstrated by the results shown above. Another factor that contributes to the lower losses calculated with AASHTO 2007 is the shape of the predicted time-history curves for creep and shrinkage (see e.g., Figs. 4.1 and 4.2). The steeper rises of the curves at the beginning will result in lower differential creep and shrinkage and, thereby, lower losses when the concrete is prestressed at a more mature age, which is often the case for post-tensioned girders. The difference in the shapes of the time-history curves predicted by the 2004 and 2007 AASHTO Specifications can be attributed to the fact that the 2004 Specifications have a time-dependent term in the formulas for the *V*/*S* factors while the 2007 Specifications do not.

4.3 Parametric Study with NW Connector of I215-CA91 Bridge

A numerical parametric study has been conducted to examine the influence of the concrete strength, the amount of mild reinforcement, the relative humidity, and the age of concrete at prestressing on the ultimate long-term prestress loss in a post-tensioned box-girder bridge. The bridge girder selected for the parametric study is the midspan section of the NW connector of the I215-CA91 bridge. The original properties of the girder section, as shown in Table 4.3, are considered the baseline values. It has a concrete strength of 6.7 ksi (47 MPa) and a total mild reinforcement ratio (ρ_{ns}) of 0.7% with respect to the net cross-sectional area of the girder, and it is subjected to an average relative humidity of 35%. The variations introduced to the values of these parameters reflect the ranges that could be found in typical post-tensioned bridge structures in California (Youakim and Karbhari 2006). For the loss calculations, the creep and shrinkage formulas recommended by AASHTO 2004 are used.

Results obtained with the refined analysis method are shown in Figs. 4.17 through 4.19. In addition, results obtained with an approximate analysis method that will be presented and discussed in Chapter 5 are also shown on the same graphs. It can be observed that increasing the relative humidity from 35 to 90% can reduce the ultimate long-term loss by as much as 7 ksi (48 MPa) when the concrete is loaded at an age of 20 days. This influence is slightly reduced as the age of concrete at loading increases. For small bridge structures with two or three spans, post-tensioning could take place within 30 days after the casting of the girders, while it could occur after 100 days for long bridge structures with many spans. As shown in the figures, this could affect the loss by as much as 5 ksi (35 MPa). The loss will be lower when the concrete is loaded at a more mature age. A similar level of loss reduction can also be observed as the amount of mild reinforcement increases from 0 to 2% of the net cross-sectional area of a girder.

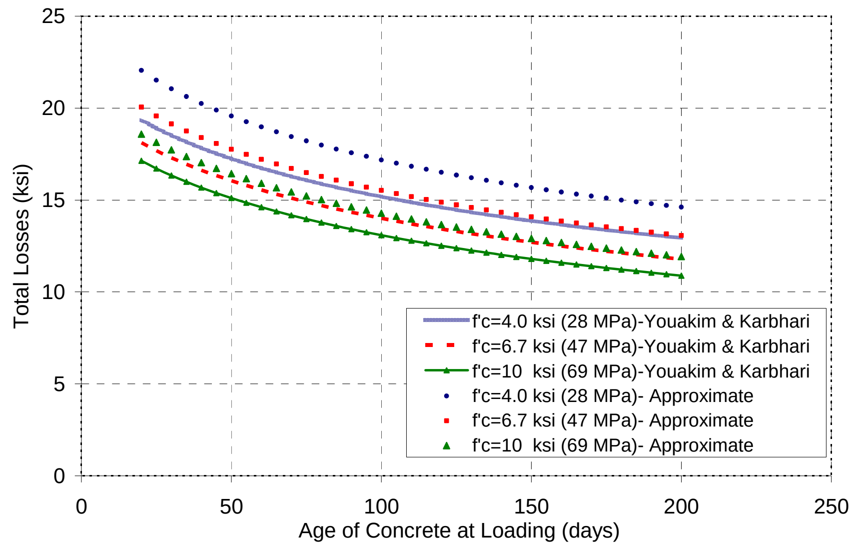

Fig. 4.17 – Influence of concrete strength

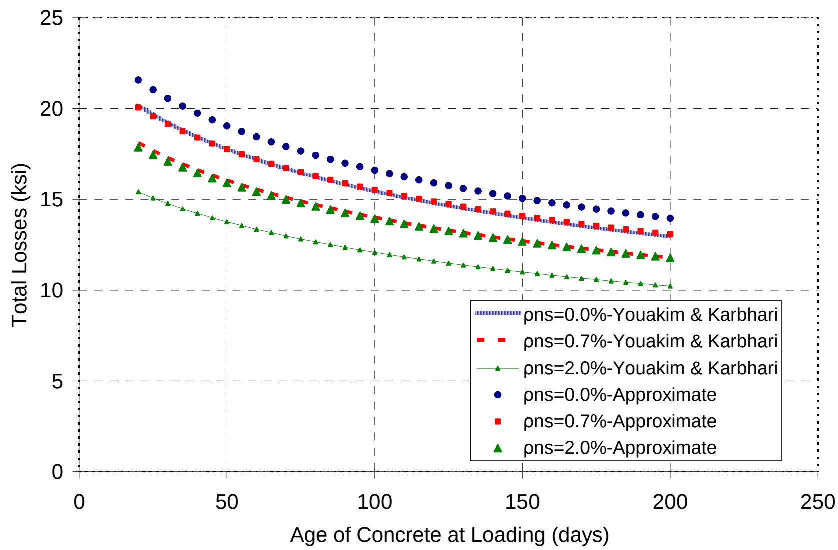

Fig. 4.18 – Influence of amount of mild reinforcement (ρ_{ns} is the ratio of the area of the total mild reinforcement to the cross-section area of the girder)

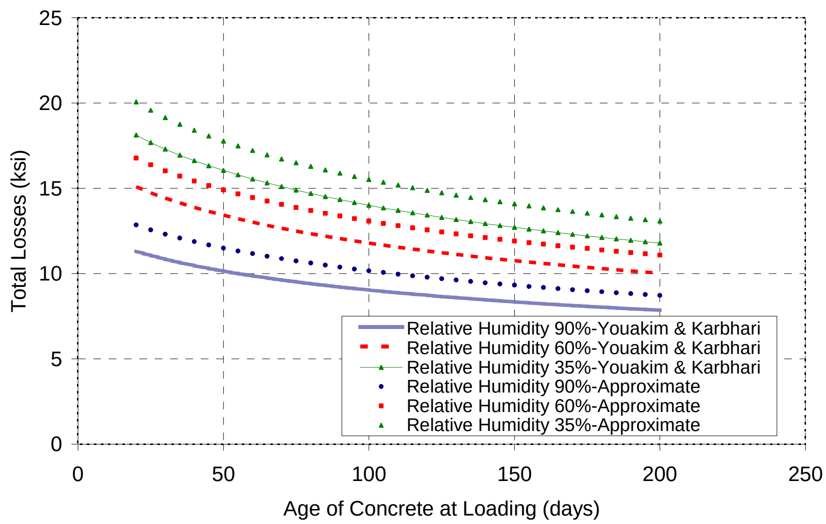

Fig. 4.19 – Influence of relative humidity

4.4 Modified Tadros' Method for Post-tensioned Girders

The refined analysis method in the AASHTO 2007/2010 LRFD Specifications for calculating long-term prestress losses is based on the study of Tadros et al. (2003), which was focused on pretensioned girders only. The basic approach used to derive this analytical method was presented in an earlier paper of Tadros et al. (1985), and was adopted by the CEB-FIP Model Code (1993). The AASHTO method does not adequately account for the influence of the mild reinforcement, and will, therefore, over-estimate losses in post-tensioned girders, which could have significantly higher amount of mild reinforcement than pretensioned girders. To address this issue, the AASHTO method has been extended in this study to account for the presence of the mild reinforcement. It will be shown that this extended method will yield practically identical results as the refined analysis method proposed by Youakim and Karbhari (2006), which has been considered in the previous sections. Since the extended AASHTO method has been derived with the same approach used by Tadros et al., it is called the modified Tadros's method in this report.

4.4.1 Creep and Shrinkage Losses

In the following derivation, the prestressing force is treated as an external force applied to the girder section, which includes the net concrete section and mild reinforcement. Furthermore, with the assumption of no bond slip, the incremental strain in the prestressing steel must be equal to that in the concrete at the same elevation.

First, the prestress loss due to the shrinkage of concrete is considered. Using the same concept as that adopted by Youakim and Karbhari (2006), the shrinkage strain that will be realized in a girder section with mild reinforcement can be calculated as $\varepsilon_{sh}(t,t_i)A_c/\bar{A}_n$, where ε_{sh} is the unrestrained shrinkage strain of concrete, A_c is the net concrete area of the girder section, and $\bar{A}_n$ is the area of the age-adjusted transformed girder section consisting of concrete and mild reinforcement only. Hence, enforcing the incremental strain compatibility condition, we have

$$\frac{\Delta f_{pS}}{E_p} = k'_A \varepsilon_{sh}(t,t_i) - \left(\frac{A_{ps}\Delta f_{pS}}{\bar{E}_c \bar{A}_n} + \frac{A_{ps}\Delta f_{pS}\bar{e}_{np}^2}{\bar{E}_c \bar{I}_n} \right) \tag{4.15}$$

where $\bar{E}_c$ is the age-adjusted modulus of elasticity of concrete defined in Eq. (4.3), and

$$k'_A = \frac{A_c}{\bar{A}_n}$$

$\bar{A}_n, \bar{I}_n$ = cross-sectional area and moment of inertia of the age-adjusted transformed girder section, which includes the net concrete area and mild reinforcement, and the transformed section is based on the age-adjusted modulus of elasticity of concrete, $\bar{E}_c$

$\bar{e}_{np}$ = eccentricity of the prestressing force with respect to centroid of the age-adjusted transformed girder section; positive when the prestressing force is below the centroid of the section

By rearranging Eq. (4.15) and taking χ to be 0.7 as in the AASHTO 2007 Specifications, we have

$$\Delta f_{pS}(t,t_i) = E_p k'_A \varepsilon_{sh}(t,t_i) K_{idn} \tag{4.16a}$$

where

$$K_{idn} = \frac{1}{1 + \frac{E_p}{E_{ci}} \frac{A_{ps}}{\bar{A}_n} \left(1 + \frac{\bar{A}_n \bar{e}_{np}^2}{\bar{I}_n}\right) \left(1 + 0.7\psi(t, t_i)\right)} \tag{4.16b}$$

with $E_{ci} = E_c(t_i)$, the modulus of elasticity of concrete at the time when the prestressing force is first applied.

For calculating the prestress loss due to the creep of concrete, three scenarios are considered for the girder section. One is the initial transformed section, which consists of the net concrete area and mild reinforcement with the modulus of elasticity of concrete taken to be E_{ci}; the second is the net concrete section, which consists of concrete only; and the third is the age-adjusted transformed section that includes the net concrete area and mild reinforcement and is calculated with the age-adjusted modulus of elasticity, $\bar{E}_c$. Following the concept used by Youakim and Karbhari (2006), we can derive the following expression for the creep strain of concrete at the location of the centroid of the prestressing steel.

$$\bar{\varepsilon}_{cp}(t, t_i) = \bar{\varepsilon}_{co}(t, t_i) - \bar{e}_{np} \bar{\phi}(t, t_i) \tag{4.17a}$$

where

$$\bar{\varepsilon}_{co}(t, t_i) = k'_A \left(\varepsilon_o(t_i) - \phi(t_i)\Delta y_1\right) \psi(t, t_i) \tag{4.17b}$$

$$\bar{\phi}(t, t_i) = k'_I \phi(t_i) \psi(t, t_i) + \frac{A_c}{\bar{I}_n} \left(\varepsilon_o(t_i) - \phi(t_i)\Delta y_1\right) \psi(t, t_i) \Delta y \tag{4.17c}$$

with $\varepsilon_o(t_i)$ and $\phi(t_i)$ being the instantaneous strain and curvature defined in Eqs. (4.6) and (4.7), Δy_1 being the distance of the centroid of the net concrete section from that of the initial transformed girder section (positive if the former is below the latter), Δy being the distance of the centroid of the age-adjusted transformed section from that of the initial transformed girder section (positive if the former is below the latter), $\bar{I}_n$ being the moment of inertia of the age-adjusted transformed section, and $k'_I = I_c / \bar{I}_n$. It should be noted that A_c and I_c are the area and moment of inertia of the net concrete section. Assuming that Δy_1 is zero, which is a good approximation, we have

$$\bar{\varepsilon}_{cp}(t,t_i)=\left(k'_A-\frac{\bar{e}_{np}A_c\Delta y}{\bar{I}_n}\right)\varepsilon_o(t_i)\psi(t,t_i)-k'_I\bar{e}_{np}\phi(t_i)\psi(t,t_i) \tag{4.18}$$

The incremental strain compatibility condition gives

$$\frac{\Delta f_{pC}}{E_p}=\bar{\varepsilon}_{cp}(t,t_i)-\left(\frac{A_{ps}\Delta f_{pC}}{\bar{E}_c\bar{A}_n}+\frac{A_{ps}\Delta f_{pC}\bar{e}_{np}^2}{\bar{E}_c\bar{I}_n}\right) \tag{4.19}$$

Substituting Eq. (4.18) into Eq. (4.19), we have

$$\Delta f_{pC}(t,t_i)=E_p\left[\left(k'_A-\frac{\bar{e}_{np}A_c\Delta y}{\bar{I}_n}\right)\varepsilon_o(t_i)-k'_I\bar{e}_{np}\phi(t_i)\right]\psi(t,t_i)K_{idn} \tag{4.20}$$

Finally, substituting Eqs. (4.6) and (4.7) into Eq. (4.20), we have

$$\Delta f_{pC}(t,t_i)=\frac{E_p}{E_{ci}}f'_{cgp}\psi(t,t_i)K_{idn} \tag{4.21a}$$

where

$$f'_{cgp}=\left(k'_A-\frac{\bar{e}_{np}A_c\Delta y}{\bar{I}_n}\right)\frac{A_{ps}f_{pi}}{A_t}-k'_I\bar{e}_{np}\frac{M_{total}}{I_t} \tag{4.21b}$$

As defined in Eqs. (4.6) and (4.7), A_t and I_t are the area and moment of inertia of the initial transformed girder section not including the prestressing steel.

It should be noted that when there is no mild reinforcement, Eqs. (4.16) and (4.21) reduce to the same expressions that are used in the refined analysis method in the AASHTO 2007 Specifications.

4.4.2 Relaxation Loss

The refined analysis method in AASHTO 2007 for calculating the relaxation loss is also based on the work of Tadros et al. (2003) for pretensioned girders, in which relaxation starts before stress transfer. For post-tensioned girders, the expression for relaxation loss can be derived in a similar fashion. Considering the incremental strain compatibility condition, we have

$$\frac{\chi_r \Delta\tilde{f}_{pR} - \Delta f_{pR}}{E_p} = \frac{A_{ps}\Delta f_{pR}}{\bar{E}_c \bar{A}_n} + \frac{A_{ps}\Delta f_{pR}\bar{e}_{np}^2}{\bar{E}_c \bar{I}_n} \tag{4.22}$$

where $\Delta\tilde{f}_{pR}$ is given in Eq. (4.13), which is a widely accepted formula for calculating relaxation loss in prestressing strands subjected to a constant tensile strain, χ_r is a reduction factor to account for the gradual reduction of the tensile strain in the prestressing strands over time due to the creep and shrinkage of concrete, A_{ps} and E_p are the total cross-sectional area and modulus of elasticity of the prestressing steel, and Δf_{pR} is the final relaxation loss realized including the elastic rebound of concrete due to relaxation. Equation (4.22) can be rewritten as

$$\Delta f_{pR} = \chi_r \Delta\tilde{f}_{pR} K_{idn} \tag{4.23}$$

where K_{idn} is defined in Eq. (4.16b). According to Tadros et al. (2003), the value χ_r can be given by the following approximation.

$$\chi_r = 1 - \frac{3(\Delta f_{pS} + \Delta f_{pC})}{f_{pi}} \tag{4.24}$$

Youakim and Karbhari (2006) have recommended that χ_r be 0.7, while it is assumed to be 0.67 in the AASHTO 2007 Specifications. However, the analysis of the bridge girders considered in this study has shown that creep and shrinkage losses in post-tensioned girders could be much less than those in pretensioned girders due to the difference in the age of concrete at prestressing and the amount of mild reinforcement. Substituting the shrinkage and creep losses calculated for the monitored bridge girders into Eq. (4.24) results in values of χ_r close to 0.8. With this value of χ_r, Eqs. (4.23) and (4.13) lead to

$$\Delta f_{pR}(t, t_i) = \frac{0.8\log(24(t - t_i))}{K'}\left(\frac{f_{pi}}{f_{py}} - 0.55\right) f_{pi} K_{idn} \tag{4.25}$$

With t assumed to be 15,000 days and K' = 45 for low-relaxation strands and 10 for other strands, the ultimate relaxation loss is then given by the following equation.

$$\Delta f_{pR} = \frac{1}{K}\left(\frac{f_{pi}}{f_{py}} - 0.55\right) f_{pi} K_{idn} \tag{4.26}$$

where K is 10 for low-relaxation strands and 2.2 for other strands.

4.5 Comparison of Refined Analysis Methods

The modified Tadros's method is compared to the method proposed by Youakim and Karbhari (2006) using the two monitored bridge structures (I5-I805 and I215-CA91). For both methods, the creep and shrinkage formulas recommended in AASHTO 2004 are used for the loss calculations. The results are shown in Figs. 4.20 through 4.27. It can be observed that the two methods yield practically identical results.

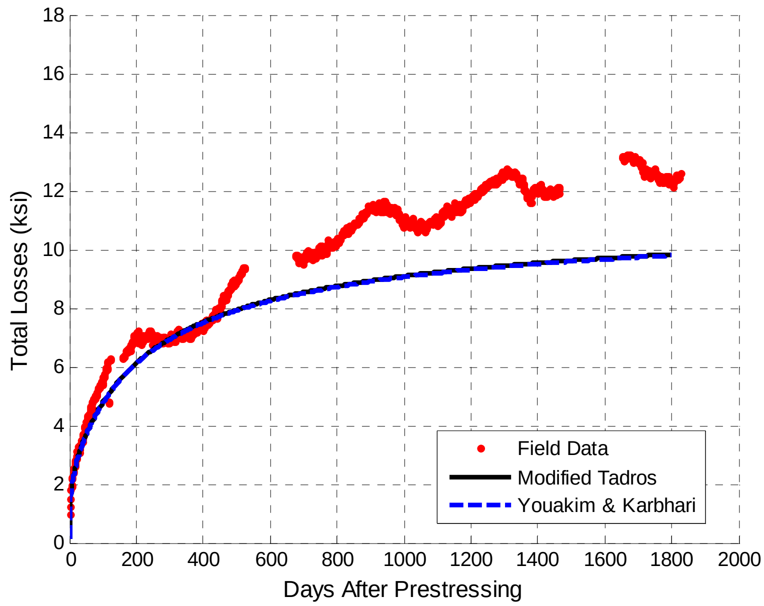

Fig. 4.20 – Total long-term prestress loss at midspan of Frame 4 of I5-I805

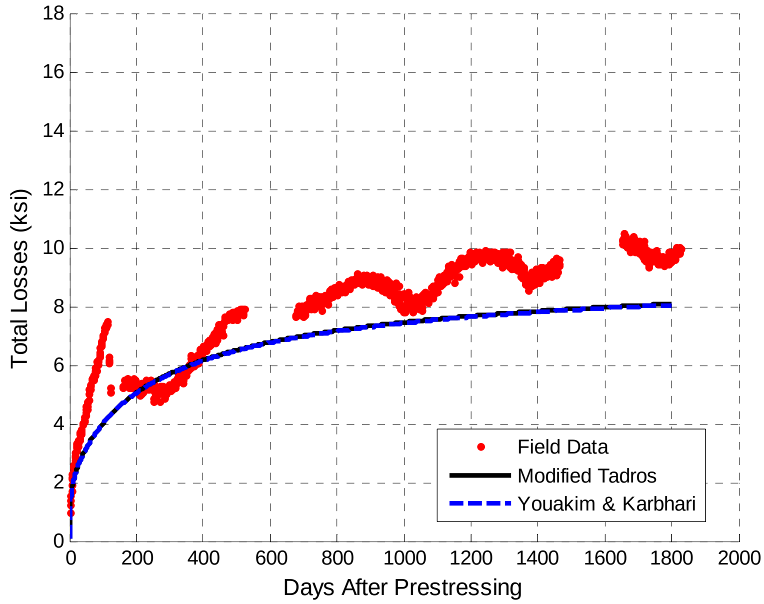

Fig. 4.21 - Total long-term prestress loss near a bent of Frame 4 in I5-I805

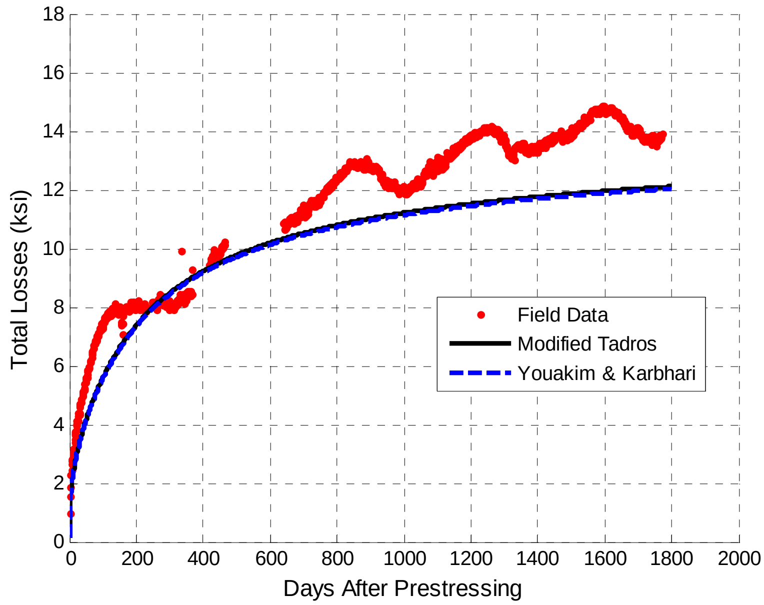

Fig. 4.22 - Total long-term prestress loss at midspan of Frame 5 in I5-I805

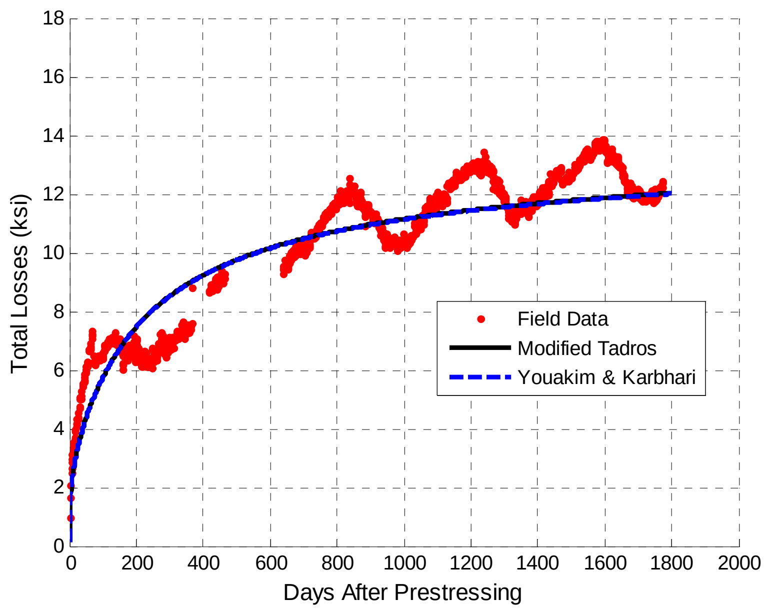

Fig. 4.23 - Total long-term prestress loss near a bent of Frame 5 in I5-I805

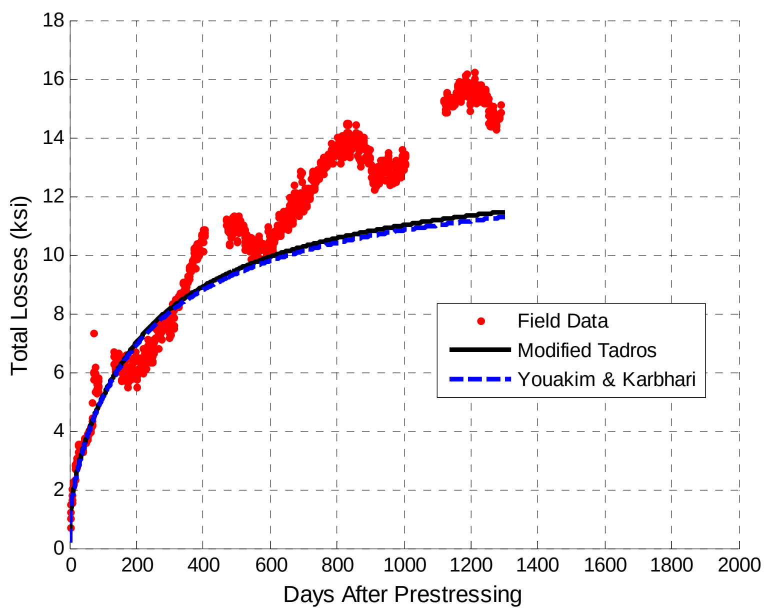

Fig. 4.24 - Total long-term prestress loss at midspan of NW connector in I215-CA91

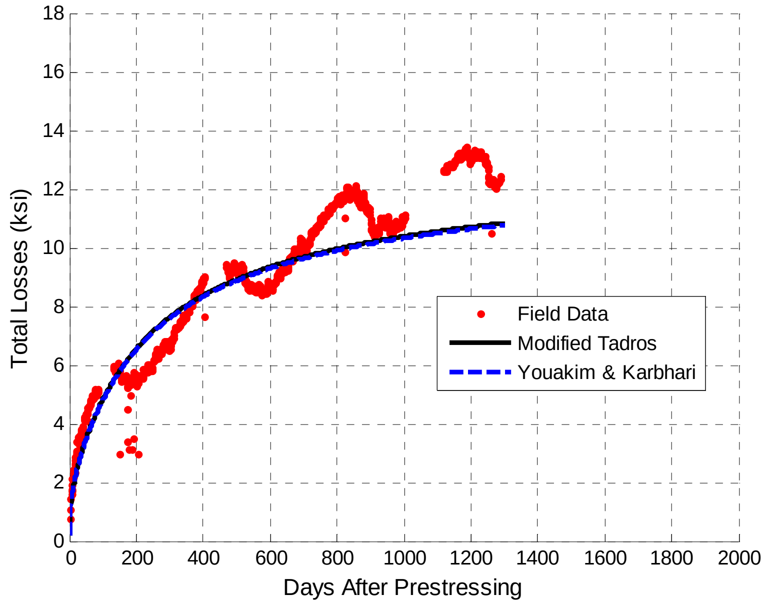

Fig. 4.25 - Total long-term prestress loss near a bent of NW connector in I215-CA91

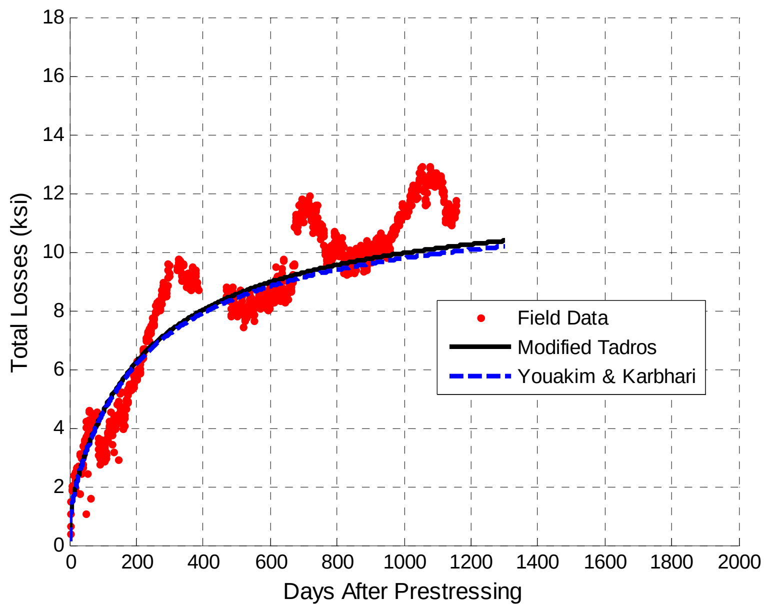

Fig. 4.26 - Total long-term prestress loss at midspan of SE connector in I215-CA91

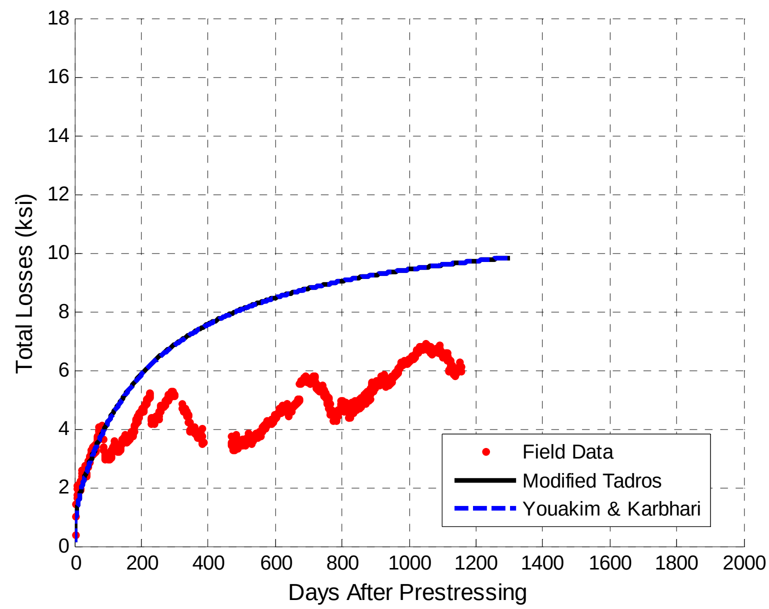

Fig. 4.27 - Total long-term prestress loss near a bent of SE connector in I215-CA91

5 Approximate Analysis Method

The approximate analysis method provided in the current (2007 and 2010) AASHTO Specifications are only applicable to pretensioned girders. A more general simplified method has been derived in this study to account for the influence of mild reinforcement and the age of concrete at prestressing, which are important factors to consider for post-tensioned girders. The derivation and validation of the method are presented in this chapter.

5.1 Derivation

Bridge girders are normally so designed that the net deflection under its self-weight and the prestressing force is minimized. Taking advantage of this condition, one may ignore the contribution of the bending deformation to estimate prestress losses. With this assumption, Eq. (4.20) for calculating the ultimate long-term creep loss can be simplified to

$$\Delta f_{pC}(\infty, t_i) = E_p k'_A \varepsilon_o(t_i)\psi(\infty, t_i)K_{idn} \tag{5.1}$$

With the expressions for k'_A in Eq. (4.15), K_{idn} in Eq. (4.16b), and the creep coefficient in Eq. 3.2 (AASHTO 2004), the above equation can be written as

$$\Delta f_{pC}(\infty, t_i) = 3.5\frac{E_p}{E_{ci}}\frac{1-\rho_{ps}-\rho_{ns}}{1+(\overline{\eta}_{ps}-1)\rho_{ps}+(\overline{\eta}_{ns}-1)\rho_{ns}}\frac{f_{pi}A_{ps}}{A_t}k_{sc}k_{hc}k_f t_i^{-0.118} \tag{5.2a}$$

where ρ_{ps} and ρ_{ns} are the respective ratios of the areas of the prestressing steel and mild reinforcement to the net cross-sectional area of the concrete girder, and

$$\overline{\eta}_{ps} = \frac{E_p}{E_{ci}}\left[1+0.7\psi(\infty, t_i)\right] \tag{5.2b}$$

$$\overline{\eta}_{ns} = \frac{E_s}{E_{ci}}\left[1+0.7\psi(\infty, t_i)\right] \tag{5.2c}$$

For most situations, one can assume that ρ_{ps} and ρ_{ns} are much less than one, $k_{sc} \approx 0.7$ with *V/S* around 5 in. or above, $\overline{\eta}_{ps} \approx \overline{\eta}_{ns}$, and $E_p / E_{ci} \approx E_s / E_{ci} \approx 6$. As a result, Eq. (5.2) can be simplified to

$$\Delta f_{pC}(\infty,t_i) = 14\frac{1}{1+(\overline{\eta}_s-1)(\rho_{ps}+\rho_{ns})}\frac{f_{pi}A_{ps}}{A_t}k_{hc}k_f t_i^{-0.118} \tag{5.3a}$$

where

$$\overline{\eta}_s = 6\left(1+1.2t_i^{-0.118}\right) \tag{5.3b}$$

Following similar assumptions as above and substituting Eq. (3.1) for the shrinkage strain (according to AASHTO 2004) into Eq. (4.16a), one has the following expression for the ultimate long-term shrinkage loss.

$$\begin{aligned}\Delta f_{pS}(\infty,t_i) = 0.51\times10^{-3}E_p\frac{1}{1+(\overline{\eta}_s-1)(\rho_{ps}+\rho_{ns})}\times \\ \left[1-\left(\frac{t_i}{35+t_i}\right)\left(\frac{45+t_i}{26e^{0.36(V/S)}+t_i}\right)\right]\left(\frac{1064-94(V/S)}{923}\right)k_{hs}\end{aligned} \tag{5.4}$$

With E_p = 28,000 ksi and by assuming that *V/S* is around 5 in., one has

$$\Delta f_{pS}(\infty,t_i) = 10\frac{1}{1+(\overline{\eta}_s-1)(\rho_{ps}+\rho_{ns})}\left(1-\frac{t_i}{35+t_i}\right)\left(\frac{45+t_i}{157+t_i}\right)k_{hs} \tag{5.5}$$

Combining Eqs. (5.3) and (5.5) and using an identical humidity correction factor, which is based on the average of k_{hc} and k_{hs}, for creep and shrinkage lead to the following approximate expression for estimating the long-term creep and shrinkage loss in post-tensioned girders.

$$\begin{aligned}\Delta f_{pC}+\Delta f_{pS} = \left[14\frac{1}{0.67+\frac{f_c'}{9}}t_i^{-0.118}\frac{f_{pi}A_{ps}}{A_t}+10\left(1-\frac{t_i}{35+t_i}\right)\left(\frac{45+t_i}{157+t_i}\right)\right]\times \\ \left(1.7-0.01H\right)\frac{1}{1+(\overline{\eta}_s-1)(\rho_{ps}+\rho_{ns})}\end{aligned} \tag{5.6}$$

The above equation has a form similar to the approximate analysis method presented in AASHTO 2007 for pretensioned members. However, it accounts for the age of concrete at prestressing and the influence of mild reinforcement in addition to the relative humidity and concrete strength. As shown by the parametric study in Section 4.3, these factors could have a major influence on long-term prestress losses.

As to the relaxation loss, one can assume 2.4 ksi for low-relaxation strands and 10 ksi for stress-relieved strands as recommended in the AASHTO 2007 Specifications.

5.2 Comparison with Refined Method

The accuracy of the approximate analysis method has been evaluated by comparing it with the modified Tadros's method. For his comparison, four bridge structures are considered. Two of them are the connectors in the I5-I805 and I215-CA91 bridges, and the other two are bridges recently designed by Caltrans engineers. One of them is the Willits Bypass, which is a single-span bridge, and the other is the Forester Creek Bridge, which has three spans. The time period used to calculate the long-term losses with the modified Tadros' method is 5,000 days.

5.2.1 I5-I805 and I215-CA91 Connectors

The girder properties for the I5-I805 and I215-CA91 connectors are given in Tables 4.1 and 4.3, respectively. The results obtained with the approximate and refined analysis methods for these two bridges are shown in Tables 5.1 and 5.2. In most cases, the approximate method gives slightly higher losses, which are a bit closer to the losses measured from the bridges. The only exception is the SE connector, for which the difference in the results is relatively significant (around 30%). For the comparison purpose, the average losses estimated with the lump-sum method in AASHTO 2007 are also shown in the tables. They are much higher than those predicted by the two analysis methods proposed here. The only design parameter considered in the lump-sum method is the partial prestressing ratio (PPR).

Table 5.1 – Comparison of approximate and refined analysis methods for I5-I805

	Prestress Losses, ksi (MPa)			
	Frame 4		Frame 5	
	Midspan	Bent	Midspan	Bent
(1) Measured (1800 days)	12.8 (88)	9.8 (68)	14.2 (98)	12.8 (88)
(2) Approximate Method	11.3 (78)	10.4 (72)	13.8 (95)	13.3 (92)
(3) Modified Tadros' Method	10.7 (74)	8.8 (61)	13.1 (91)	13.1 (90)
[(2)-(3)]/(3)x100	6	18	4	2
AASHTO Lump Sum	17.8 (151)	17.8 (151)	17.4 (150)	17.4 (150)

Table 5.2 - Comparison of approximate and refined analysis methods for I215-CA91

	Prestress Losses, ksi (MPa)			
	NW Connector		SE Connector	
	Midspan	Bent	Midspan	Bent
(1) Measured (1200 days)	15.2 (105)	12.5 (86)	12.2 (84)	6.5 (45)
(2) Approximate Method	14.1 (97)	13.5 (93)	14.8 (102)	14.3 (99)
(3) Modified Tadros' Method	12.9 (90)	12.4 (85)	11.7 (81)	11.1 (77)
[(2)-(3)]/(3)x100	9	9	27	29
AASHTO Lump Sum	18.0 (152)	18.0 (152)	17.8 (150)	17.8 (150)

5.2.2 Willits Bypass and Forester Creek Bridge

Willits Bypass is a single-span bridge with a span length of 160 ft. (48 m). It is to be located in a coastal town, Willits, midway between San Francisco and Eureka. The design of the bridge is shown in Fig. 5.1, and the girder properties obtained from the design drawings of Caltrans are summarized in Table 5.3. Both the midspan section and a section near an abutment are considered.

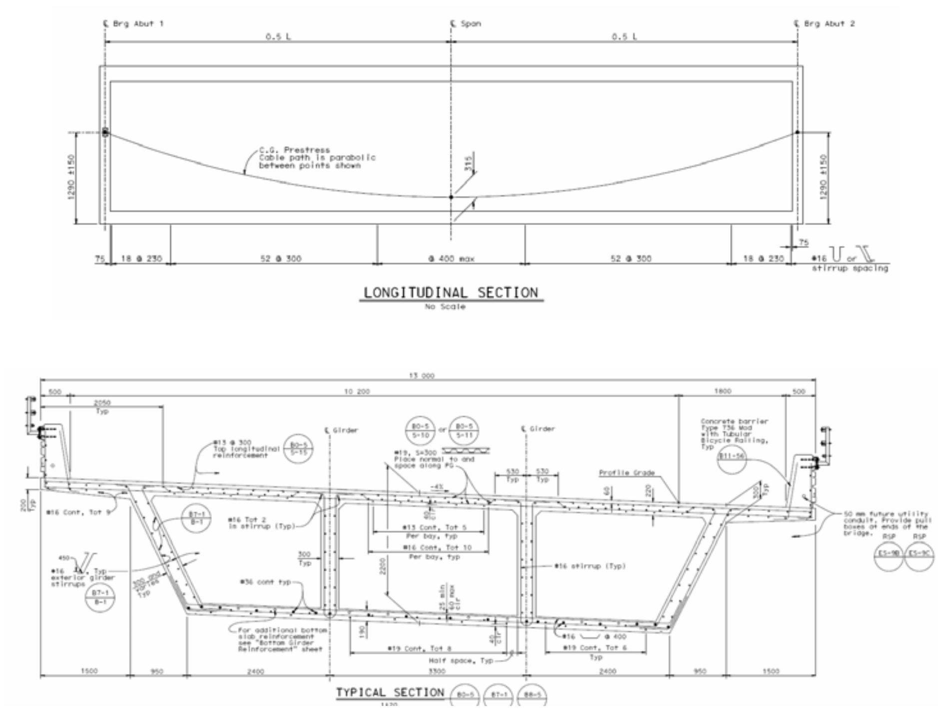

Fig. 5.1 – Willits bypass single-span bridge (Caltrans design drawings)

Table 5.3 - Girder properties for Willits Bypass bridge

Input Parameters	Willits	
	Midspan	Abutment
Girder cross-sectional area, in.^{2} (m^2)	10,060 (6.49)	10,060 (6.49)
Concrete Young's modulus, ksi (GPa)	4,119 (28.40)	4,119 (28.40)
Volume-to-surface ratio, *V*/*S*, in. (mm)	5.00 (127)	5.00 (127)
Age coefficient, χ	0.70	0.70
Concrete age at end of curing, days	7	7
Concrete age at prestressing, days	30	30
Mild reinforcement Young's modulus, ksi (GPa)	29,000 (200)	29,000 (200)
Prestressing steel Young's modulus, ksi (GPa)	28,000 (193)	28,000 (193)
Area of prestressing steel, in.^{2} (cm^2)	52.8 (341)	52.8 (341)
Distance of prestressing steel from top surface, in. (m)	74.4 (1.89)	35.8 (0.91)
Prestressing force, kips (kN)	10,690 (47,550)	10,690 (47,550)
Moment (due to self-weight & prestressing), kip-in (kN-m)	20,657 (2,334)	0
Relative humidity, %	80	80
Specified 28-day concrete strength, ksi (MPa)	5.08 (35.0)	5.08 (35.0)
Top mild reinforcement area, in.^{2} (cm^2)	23.0 (149)	23.0 (149)
Bottom mild reinforcement area, in.^{2} (cm^2)	78.2 (505)	65.6 (423)
Girder cross-sectional area, in.^{2} (m^2)	10,056 (6.49)	10,056 (6.49)
Distance of centroidal axis of concrete section from top surface, in. (m)	35.8 (0.91)	35.8 (0.91)
Span length, in. (m)	1,929 (49.0)	

The Forester Creek Bridge has three spans, with the middle span 182-ft. (55.5-m) long. It is to be located in El Cajon, which is about 30 miles (48 km) from the San Diego coast. The design of the bridge structure is shown in Fig. 5.2, and the girder properties for the midspan section and a section near a bent of the middle span, which is considered here, are given in Table 5.4.

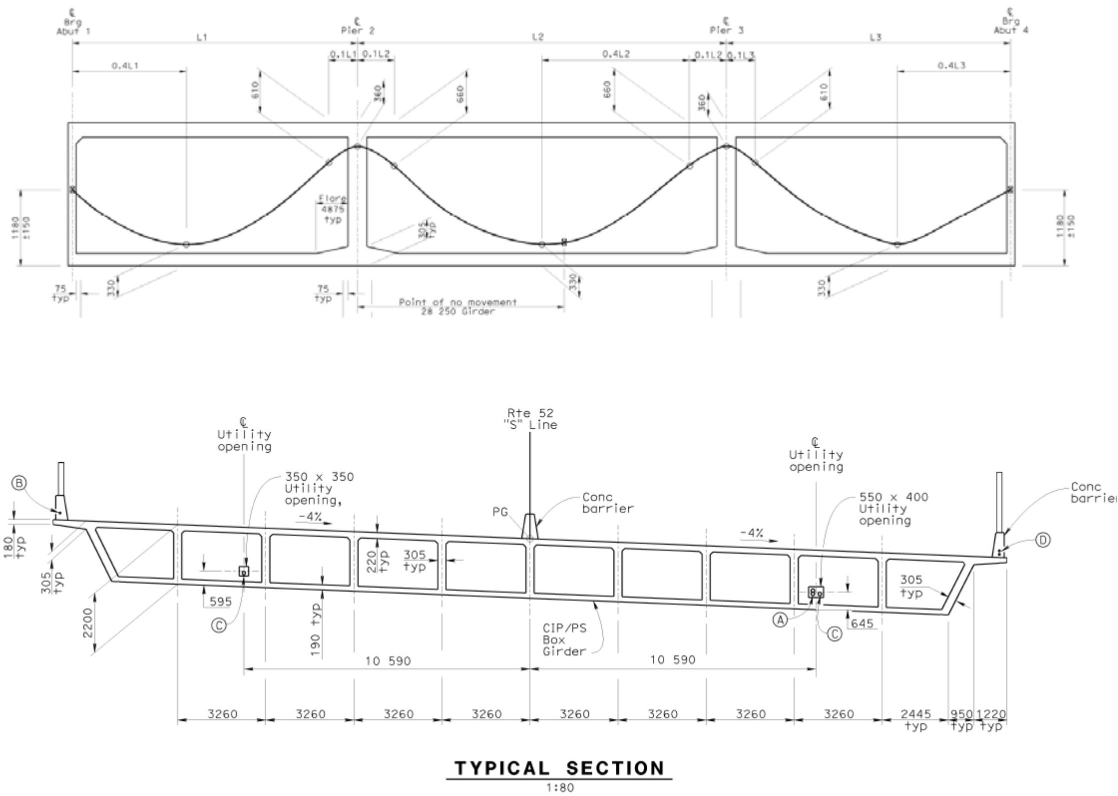

Fig. 5.2 – Forester Creek three-span bridge (Caltrans design drawings)

The long-term prestress losses calculated with the approximate analysis method and the modified Tadros's method for both bridges are compared in Table 5.5. It can be observed that the approximate analysis method gives slightly smaller losses with a maximum discrepancy of 16%. The values given by the lump-sum method in AASHTO 2007 are also shown in the table.

Table 5.4 - Girder properties for Forester Creek bridge

Input Parameters	Forester	
	Midspan	Bent
Girder cross-sectional area, in.^{2} (m^2)	34,674 (22.37)	34,674 (22.37)
Concrete Young's modulus, ksi (GPa)	3,876 (26.73)	3,876 (26.73)
Volume-to-surface ratio, *V/S*, in. (mm)	5.00 (127)	5.00 (127)
Age coefficient, χ	0.70	0.70
Concrete age at end of curing, days	7	7
Concrete age at prestressing, days	30	30
Mild reinforcement Young's modulus, ksi (GPa)	29,000 (200)	29,000 (200)
Prestressing steel Young's modulus, ksi (GPa)	28,000 (193)	28,000 (193)
Area of prestressing steel, in.^{2} (cm^2)	96.4 (622)	96.4 (622)
Distance of prestressing steel from top surface, in. (m)	73.6 (1.87)	14.2 (0.36)
Prestressing force, kips (kN)	19,510 (86,785)	19,510 (86,785)
Moment (due to self-weight & prestressing), kip-in (kN-m)	243,520 (27,515)	-38,6138 (-43,630)
Relative humidity, %	65	65
Specified 28-day concrete strength, ksi (MPa)	4.50 (31.0)	4.50 (31.0)
Top mild reinforcement area, in.^{2} (cm^2)	87.2 (562)	117.6 (759)
Bottom mild reinforcement area, in.^{2} (cm^2)	35.4 (228)	35.4 (228)
Girder cross-sectional area, in.^{2} (m^2)	34,680 (22.37)	34,680 (22.37)
Distance of centroidal axis of concrete section from top surface, in. (m)	36.2 (0.92)	36.2 (0.92)
Span length, in. (m)	2,185 (55.5)	

Table 5.5 - Comparison of approximate and refined analysis methods for Willits and Forester bridges

	Prestress Losses, ksi (MPa)			
	Willits Bridge		Forester Bridge	
	Midspan	Abutment	Midspan	Bent
Approximate Method	14.8 (102)	14.9 (103)	14.8 (102)	14.7 (101)
Modified Tadros' Method	15.5 (107)	17.3 (119)	14.8 (102)	15.2 (105)
Difference in %	-5	-13	0	-4
AASHTO Lump Sum	17.7 (150)	17.8 (150)	18.0 (152)	17.8 (150)

5.3 Parametric Study

The parametric study conducted in Section 4.3 has been repeated using the approximate analysis method. The results are shown in Figs. 4.17 through 4.19. It can be observed that the trend of variation of the prestress loss with respect to the change in the various parameters is similar to that obtained with the refined analysis method of Youakim and Karbhari. The approximate method well captures the influence of these parameters.

6 Proposed Changes to AASHTO Specifications

The modified Tadros' method, presented in Section 4.4 of this report, and the approximate analysis method, presented in Chapter 5, will now be expressed in such forms that they can be readily implemented in the AASHTO LRFD Bridge Design Specifications. They are not intended to replace the current prestress-loss estimation methods in AASHTO but to extend the current AASHTO Specifications to cover post-tensioned members.

6.1 Proposed Refined Analysis Method for Post-tensioned Girders

6.1.1 Creep and Shrinkage of Concrete

For the proposed refined analysis method, the following formulas, taken from the 2004 AASHTO LRDF Specifications, should be used to calculate the shrinkage and creep of concrete. They have provided a much better correlation to the material and prestress-loss data obtained from the two monitored bridge structures than the formulas given in the AASHTO 2007 Specifications, as shown in Sections 3.3 and 4.2 of this report. The formulas in AASHTO 2007 are, to a large extent, based on data obtained from high-strength concrete and with specimens cured at an ambient room temperature of 73^{o}F (23 ^{o}F) and loaded one day after casting. For post-tensioned girders, loading could take place a long while (30 days or more) after casting. Furthermore, the formulas in the 2007 Specifications ignore the time-dependent terms in the *V*/*S* correction factors for creep and shrinkage. This affects the shape of the time-history curves for creep and shrinkage, and leads to an under-estimation of the differential creep and shrinkage when the concrete is not prestressed within the first few days of casting but at a more mature age, as discussed in Section 4.2.3.

The AASHTO 2004 LRDF Specifications for shrinkage and creep, as presented in Section 3.1, are repeated below.

Shrinkage

$$\varepsilon_{sh}(t) = k_{ss} k_{hs} k_{tds} \times 0.51 \times 10^{-3} \tag{6.1a}$$

where

$$k_{ss} = \left[\frac{\dfrac{t}{26e^{0.36(V/S)} + t}}{\dfrac{t}{45 + t}} \right] \left[\frac{1064 - 94(V/S)}{923} \right] \tag{6.1b}$$

$$k_{hs} = \frac{140 - H}{70} \text{ for } H < 80\% \text{ and } \frac{3(100 - H)}{70} \text{ for } H \geq 80\% \tag{6.1c}$$

$$k_{tds} = \frac{t}{35 + t} \tag{6.1d}$$

with

t = days from end of curing

V/S = volume-to-surface area ratio (in.) with a maximum allowable value of 6 in.

H = relative humidity (%)

Creep

$$\psi(t, t_i) = 3.5 k_{sc} k_{hc} k_f k_{tdc} t_i^{-0.118} \tag{6.2a}$$

where

$$k_{sc} = \left[\frac{\dfrac{t - t_i}{26e^{0.36(V/S)} + (t - t_i)}}{\dfrac{(t - t_i)}{45 + (t - t_i)}} \right] \left[\frac{1.80 + 1.77e^{-0.54(V/S)}}{2.587} \right] \tag{6.2b}$$

$$k_{hc} = 1.58 - \frac{H}{120} \tag{6.2c}$$

$$k_f = \frac{1}{0.67 + \dfrac{f'_c}{9}} \tag{6.2d}$$

$$k_{tdc} = \frac{(t - t_i)^{0.6}}{10 + (t - t_i)^{0.6}} \tag{6.2e}$$

with

t = age of concrete (days)

t_i = age of concrete at prestressing or load application (days)

f_c' = compressive strength of concrete at 28 days (ksi)

6.1.2 Total Long-Term Loss

The total ultimate long-term loss Δf_{pLT} can be calculated as the sum of the ultimate shrinkage loss Δf_{pS}, creep loss Δf_{pC}, and relaxation loss Δf_{pR}.

$$\Delta f_{pLT} = \Delta f_{pS} + \Delta f_{pC} + \Delta f_{pR} \tag{6.3}$$

The formula for calculating each loss component is presented below.

Shrinkage Loss

Based on Eq. (4.16), the ultimate long-term prestress loss due to concrete shrinkage is given by

$$\Delta f_{pS} = E_p k_A' \Delta\varepsilon_{sh} K_{idn} \tag{6.4}$$

where

$\Delta\varepsilon_{sh} = \varepsilon_{sh}(\infty) - \varepsilon_{sh}(t_i)$

E_p = modulus of elasticity of the prestressing steel

$k_A' = \dfrac{A_c}{\bar{A}_n}$

$$K_{idn} = \frac{1}{1 + \dfrac{E_p}{E_{ci}} \dfrac{A_{ps}}{\bar{A}_n} \left(1 + \dfrac{\bar{A}_n \bar{e}_{np}^2}{\bar{I}_n}\right)\left(1 + 0.7\psi(\infty, t_i)\right)}$$

with

E_{ci} = modulus of elasticity of concrete at the time of prestressing

A_{ps} = cross-sectional area of the prestressing steel

A_c = cross-sectional area of the net concrete section

$\overline{A}_n, \overline{I}_n$ = cross-sectional area and moment of inertia of the age-adjusted transformed girder section, which includes the net concrete area and mild reinforcement; the transformed section is based on the age-adjusted modulus of elasticity of concrete, $\overline{E}_c = E_{ci} / \left(1 + 0.7\psi(\infty, t_i)\right)$

$\overline{e}_{np}$ = eccentricity of the prestressing force with respect to the centroid of the age-adjusted transformed girder section; positive when the prestressing force is below the centroid of the section

Creep Loss

Based on Eq. (4. 20), the ultimate long-term prestress loss due to the creep of concrete is given by

$$\Delta f_{pC} = \frac{E_p}{E_{ci}} f'_{cgp} \psi(\infty, t_i) K_{idn} \tag{6.5}$$

where

$$f'_{cgp} = \left(k'_A - \frac{\overline{e}_{np} A_c \Delta y}{\overline{I}_n} \right) \frac{A_{ps} f_{pi}}{A_t} - k'_I \overline{e}_{np} \frac{M_{total}}{I_t}$$

with

Δy = distance of the centroid of the age-adjusted transformed section from that of the initial transformed girder section; positive if the former is below the latter

$$k_I' = \frac{I_c}{I_n}$$

I_c = moment of inertia of the net concrete section

A_t, I_t = cross-sectional area and moment of inertia of the initial transformed girder section, which includes the net concrete area and mild reinforcement; the transformed section is based on the initial modulus of elasticity of concrete, E_{ci}

f_{pi} = initial prestress right after stress transfer

M_{total} = total moment at the girder section right after post-tensioning; it is usually the sum of moments induced by the self-weight and the equivalent load of the prestressing force

Relaxation Loss

The relaxation loss can be evaluated with the following equation as derived in Section 4.3.2.

$$\Delta f_{pR} = \frac{1}{K}\left(\frac{f_{pi}}{f_{py}} - 0.55\right) f_{pi} K_{idn} \tag{6.6}$$

where

K = 10 for low-relaxation strands and 2.2 for other strands

f_{py} = yield strength of the prestressing steel

6.2 Approximate Analysis Method

The approximate analysis method has been derived in Chapter 5. It may be used to calculate the total ultimate long-term loss in lieu of the refined analysis method. With Eq. (5.6) and a simple approximation for the relaxation loss, the total ultimate long-term loss can be calculated as

$$\Delta f_{pLT} = \left(14\gamma_{st}\gamma_{ac}(t_i)\frac{f_{pi}A_{ps}}{A_t} + 10\gamma_{as}(t_i)\right)\gamma_h\gamma_{sr} + \Delta f_{pR} \tag{6.7}$$

where

$$\gamma_{st} = \frac{1}{0.67 + \frac{f_c'}{9}}$$

$f_c' =$ 28-day compresssive strength of concrete (ksi)

$$\gamma_{ac}(t_i) = t_i^{-0.118}$$

$$\gamma_{as}(t_i) = 1 - \left(\frac{t_i}{35 + t_i}\right) \times \left(\frac{45 + t_i}{157 + t_i}\right)$$

$$\gamma_h = 1.7 - 0.01H$$

$$\gamma_{sr} = \frac{1}{1 + (\overline{\eta}_s - 1)(\rho_{ns} + \rho_{ps})}$$

ρ_{ns} = ratio of total mild reinforcement with respect to the net cross-sectional area of the girder section

ρ_{ps} = ratio of prestressing steel with respect to the net cross-sectional area of the girder section

$$\overline{\eta}_s = 6\left(1 + 1.2t_i^{-0.118}\right)$$

$\Delta f_{pR} = 2.4$ ksi for low-relaxation strands and 10 ksi for stress-relieved strands

6.3 Design Procedure

The use of the aforementioned analysis methods in design requires a few iteration cycles as described below.

1. Use the approximate analysis method to estimate the total prestress loss.

a. Specify the 28-day compressive strength of the concrete to be used.

b. Determine the average relative humidity for the site where the bridge will be located.

c. Estimate the time t_i at which post-tensioning will take place.

d. Estimate the quantities of prestressing steel and mild reinforcement to be used.

e. Assume $f_{pi} A_{ps} / A_t = 0.15 f_c'$.

f. Calculate $\Delta f_{pLT} / f_{pj}$ using Eq. (6.7) and the jacking stress f_{pj} permitted by the AASHTO Specifications.

2. Determine the required concrete strength, initial prestressing force, and amount of prestressing steel.

3. Revise the loss estimate with the f_c', A_{ps}, and f_{pi} determined in Step 2 using either the approximate or refined analysis method.

4. Go to Step 2 and repeat the process if the revised loss estimate differs significantly from that obtained in the previous cycle.

5. Otherwise, the design is satisfactory.

7 Conclusions

The current AASHTO LRFD Bridge Design Specifications (2007 and 2010) do not provide adequate methods for calculating long-term prestress losses in post-tensioned members. The analysis methods provided in the specifications are essentially based on research focused on pretensioned girders. In this study, a refined analysis method proposed by Youakim and Karbhari (2006) for estimating long-term losses in post-tensioned girders has been evaluated, and a new refined analysis method has been developed. Both methods have been validated with field data collected from two bridge structures that were monitored for long-term prestress losses over a duration of more than four years. One bridge is located in a coastal area in San Diego, California, and the other is located inland in Riverside, California. Creep and shrinkage data were obtained from concrete cylinders prepared with the same batches of concrete used for the monitored bridge girders. The two methods considered here have been shown to produce practically identical results, but the new analysis method proposed here has a form similar to the refined analysis method provided in the current AASHTO Specifications.

The formulas recommended in the AASHTO 2004 and 2007 Specifications for calculating the creep and shrinkage of concrete have been evaluated with the material data obtained and they have been used for the loss calculations. The formulas recommended in AASHTO 2004 have provided a much better correlation to the creep and shrinkage values obtained from the concrete cylinders than those in AASHTO 2007. In general, the AASHTO 2007 formulas significantly under-estimate the creep and shrinkage of the concrete cylinders.

Discounting the abnormal prestress-loss values obtained from one girder section, the maximum difference between the long-term losses calculated with the refined analysis methods and the collected field data is no more than 16% when the measured creep and shrinkage properties of the concrete are used for the calculations. The maximum difference increases to 27% when the creep and shrinkage predicted by AASHTO 2004 are used, and to 49% when the creep and shrinkage predicted by AASHTO 2007 are used.

An approximate analysis method has also been developed in this study. This method accounts for the presence of mild reinforcement, the age of concrete at prestressing, the relative humidity the structure is exposed to, and the compressive strength of concrete. It is, therefore, suitable for post-tensioned bridge girders. The method assumes a form that is similar to the approximate analysis method in the current AASHTO Specifications for pretensioned members.

It has been validated with the proposed refined analysis method using six bridge girders, including four from the two monitored bridge structures. Except for one girder, the values obtained from the refined and approximate analysis methods differ by no more than 16%. For one girder, the difference is about 30%.

A numerical parametric study has been conducted on one of the monitored girder sections to examine the influence of the concrete strength, the amount of mild reinforcement, the relative humidity, and the age of concrete at prestressing on the ultimate long-term prestress loss in a post-tensioned box-girder bridge. It has been observed that changing the relative humidity from 35 to 90% reduces the ultimate long-term loss by 7 ksi (48 MPa). Furthermore, the age of concrete at post-tensioning could also make a difference. Changing the post-tensioning age from 30 to 100 days reduces the loss by about 5 ksi (35 MPa). A similar level of loss reduction can also be observed as the amount of mild reinforcement increases from 0 to 2% of the net cross-sectional area of a girder.

Both the refined and approximate analysis methods proposed here are in forms that can be readily implemented in the AASHTO LRFD Specifications. Suggestions for their implementation are provided in this report. Information on the relative humidity is important for an accurate assessment of creep and shrinkage losses. This information is provided in a contour map in the AASHTO LRFD Specifications at a relatively coarse scale. However, more accurate relative humidity information for specific sites can be found on local climate websites.

The rate of prestress losses in the two monitored bridges has been leveling off after a period of four years but has not approached zero. The latest measured losses have still shown a trend of very slow increase with time. Since the monitoring instruments are still in the two bridge structures, it will be worthwhile to continue data collection for a period of two additional years.

REFERENCES

AASHTO (2004). *AASHTO LRFD Bridge Design Specifications*. Third Edition, American Association of State Highway and Transportation Officials, Washington, D.C.

AASHTO (2007). *AASHTO LRFD Bridge Design Specifications*. Fourth Edition, American Association of State Highway and Transportation Officials, Washington, D.C.

AASHTO (2010). *AASHTO LRFD Bridge Design Specifications*. Fifth Edition, American Association of State Highway and Transportation Officials, Washington, D.C.

Bazant, Z.P. (1972). "Prediction of Creep Effects using Age-Adjusted Effective Modulus Method." *ACI Journal*, 69(4), 212-217.

CEB-FIP (1993). *Model Code for Concrete Structures*. CEB-FIP MC 90, Comité Euro-International du Beton – Fédération Internationale de la Précontrainte, Lausanne, Switzerland.

Ghali, A. Favre, R., and Elbadry, M.M. (2002). *Concrete Structures: Stresses and Deformations*. Third Edition, E & FN Spon Press, London & New York.

Kim, S.D. (2009). "Prediction of Long-Term Prestress Loss in Concrete Box Girder Bridges.", *PhD Dissertation*, Department of Structural Engineering, University of California at San Diego, La Jolla, CA.

Lewis, M. and Karbhari, V.M. (2006). "Experimental Verification of the Influence of Time-Dependent Material Properties on Long-Term Bridge Characteristics." *Report No. SSRP-06/01*, Department of Structural Engineering, University of California at San Diego, La Jolla, CA.

Tadros, M.K., Al-Omaishi, N., Seguirant, S.J., and Gallt, J.G. (2003). "Prestress Losses in Pretensioned High-Strength Concrete Bridge Girders." *NCHRP Report 496*, National Cooperative Highway Research Program, Transportation Research Board, Washington, D.C.

Tadros, M.K., Ghali, A., and Meyer, A.W. (1985). "Prestress Loss and Deflection of Precast Concrete Members." *PCI Journal*, Vol. 30(1), 114-141.

Youakim, S. and Karbhari, V.M. (2006). “A Simplified Method for Prediction of Long-Term Prestress Loss in Post-Tensioned Concrete Bridges.” *Report No. SSRP-06/21*, Department of Structural Engineering, University of California at San Diego, La Jolla, CA.